Spring 1982

A CHARACTERIZATION OF THE BACTERIOPHAGE 41C AND ITS LYTIC CYCLE IN BACILLUS SUBTILIS 168

DENISE MARATEA

INFORMATION TO USERS

This reproduction was made from a copy of a document sent to us for microfilming. While the most advanced technology has been used to photograph and reproduce this document, the quality of the reproduction is heavily dependent upon the quality of the material submitted.

The following explanation of techniques is provided to help clarify markings or notations which may appear on this reproduction.

1. The sign or "target" for pages apparently lacking from the document photographed is "Missing Page(s)". If it was possible to obtain the missing page(s) or section, they are spliced into the film along with adjacent pages. This may have necessitated cutting through an image and duplicating adjacent pages to assure complete continuity.

2. When an image on the film is obliterated with a round black mark, it is an indication of either blurred copy because of movement during exposure, duplicate copy, or copyrighted materials that should not have been filmed. For blurred pages, a good image of the page can be found in the adjacent frame. If copyrighted materials were deleted, a target note will appear listing the pages in the adjacent frame.

3. When a map, drawing or chart, etc., is part of the material being photographed, a definite method of "sectioning" the material has been followed. It is customary to begin filming at the upper left hand corner of a large sheet and to continue from left to right in equal sections with small overlaps. If necessary, sectioning is continued again—beginning below the first row and continuing on until complete.

4. For illustrations that cannot be satisfactorily reproduced by xerographic means, photographic prints can be purchased at additional cost and inserted into your xerographic copy. These prints are available upon request from the Dissertations Customer Services Department.

5. Some pages in any document may have indistinct print. In all cases the best available copy has been filmed.

University Microfilms International
300 N. Zeeb Road
Ann Arbor, MI 48106

Maratea, Denise

A CHARACTERIZATION OF THE BACTERIOPHAGE 41C AND ITS LYTIC CYCLE IN BACILLUS SUBTILIS 168

University of New Hampshire PH.D. 1982

PLEASE NOTE:

In all cases this material has been filmed in the best possible way from the available copy. Problems encountered with this document have been identified here with a check mark ✓.

1. Glossy photographs or pages ✓
2. Colored illustrations, paper or print _____
3. Photographs with dark background ✓
4. Illustrations are poor copy _____
5. Pages with black marks, not original copy _____
6. Print shows through as there is text on both sides of page _____
7. Indistinct, broken or small print on several pages ✓
8. Print exceeds margin requirements _____
9. Tightly bound copy with print lost in spine _____
10. Computer printout pages with indistinct print _____
11. Page(s) _____ lacking when material received, and not available from school or author.
12. Page(s) _____ seem to be missing in numbering only as text follows.
13. Two pages numbered _____. Text follows.
14. Curling and wrinkled pages _____
15. Other _____

A CHARACTERIZATION OF THE BACTERIOPHAGE 41c AND ITS LYTIC CYCLE IN *BACILLUS SUBTILIS* 168

BY

Denise Maratea
B.S., State College at Boston, 1977
M.S., University of New Hampshire, 1979

DISSERTATION

Submitted to the University of New Hampshire
in Partial Fulfillment of
the Requirements for the Degree of

Doctor of Philosophy
in
Microbiology

May, 1982

This dissertation has been examined and approved.

Dissertation director, David L. Balkwill, Assistant Professor of Microbiology

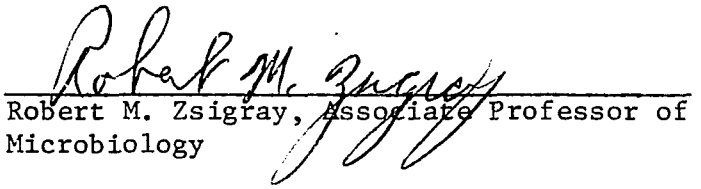

Robert M. Zsigray, Associate Professor of Microbiology

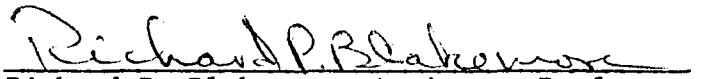

Richard P. Blakemore, Assistant Professor of Microbiology

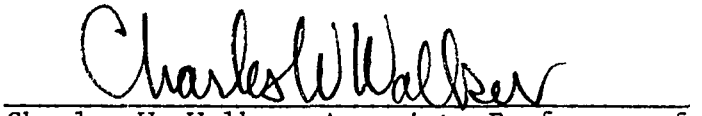

Charles W. Walker, Associate Professor of Zoology

William C. Ghiorse, Assistant Professor of Microbiology, Cornell University

ACKNOWLEDGEMENTS

The author expresses her unfeigned gratitude to Dr. David L. Balkwill. His dedication and assistance were major factors in the completion of this dissertation. I am indebted to Dr. Robert M. Zsigray for his expert guidance and many useful suggestions. I also thank Dr. Richard P. Blakemore, Dr. Charles W. Walker, and Dr. William Ghiorse (Cornell University) for serving on the dissertation committee.

Michael Warshaver and Robert Mooney provided invaluable technical assistance. This dissertation was supported by the University of New Hampshire through a dissertation fellowship and a CURF (Central University Research Fund) grant.

I am especially grateful to my parents. The faith and love they provided will always be an inspiration. Finally, I thank Donna, a dear friend, who was a constant source of encouragement.

TABLE OF CONTENTS

LIST OF TABLES

LIST OF FIGURES

ABSTRACT

A CHARACTERIZATION OF THE BACTERIOPHAGE 41c AND ITS LYTIC CYCLE IN *BACILLUS SUBTILIS* 168

by

DENISE MARATEA

University of New Hampshire, May, 1982

The ultrastructure of the lytic cycle of phage 41c in *Bacillus subtilis* 168 was examined by transmission electron microscopy. Thin sections of phage 41c-infected cells revealed that, prior to the appearance of phage structures, a marked rearrangement of the tightly packed, vesicular mesosomes was usually seen within the host cells. These mesosomes opened up into loosely arranged, lamellar forms. As phage accumulated, they appeared to be preferentially associated with the mesosomes. Towards the later portion of the lytic cycle, the mesosomes took on distinctive, loosely organized, spiral configurations. These ultrastructural changes occurred even in the presence of chloramphenicol, indicating that protein synthesis was not responsible for the alterations. Since it was possible that phage assembly was mesosome associated, infected cells were treated with lysozyme to form protoplasts. However, phage were never found within the extruded mesosomes. Furthermore, phage replication occurred in protoplasts, although the burst size was decreased. Sucrose-stabilized protoplasts only produced a burst of 1-2% of that in whole cells, while sorbitol-stabilized protoplasts produced a burst of 25-30% of that in whole cells.

Results of energy-dispersive X-ray analysis indicated less potassium and phosphorous in infected cells than in noninfected cells. These results suggested that the mesosome alterations may have occurred due to differences in the ionic composition of the cells.

A characterization study of phage 41c was also conducted. Phage 41c produced a burst size of 10^3 phage per host cell, following a latent period of 50 minutes. In addition, phage 41c (a double-stranded DNA phage) was found to be remarkably similar to another B. subtilis phage, SPP1. They were almost identical in size, morphology, sensitivity of infection to deoxyribonuclease or streptomycin, plaquing efficiency, host range, and incorporation of ^{3}H-thymidine into their DNA. Differences were detected in the molecular weights of their structural proteins and in their plaque morphologies. Phage SPP1 produced a series of changes in the ultrastructure of the host cell which was identical to that of 41c-infected cells. In contrast, a dissimilar phage, SP82G, did not produce such changes in the host cells.

I. INTRODUCTION

Bacteriophage 41c is a double-stranded deoxyribonucleic acid (DNA) virus of Bacillus subtilis (93). Morphologically, it is identical in structure and dimensions to the B. subtilis bacteriophage SPP1. Both are lytic phages and possess icosahedral heads and non-contractile tails. Phage 41c is unique in at least two aspects of its infection cycle. Infection is sensitive to treatment with deoxyribonuclease (93) and calcium is required for efficient replication (41) of the phage.

An ultrastructural examination of B. subtilis phage interactions during the lytic cycle with either 41c or SPP1 revealed a consistent and orderly rearrangement of host mesosomes (intracellular membranes), during infection. Although the ultrastructural aspects of virus infection in Gram-negative bacteria have been well documented, there have been few detailed studies for Gram-positive organisms. Consequently, an alteration of mesosomes during phage infection of Gram-positive cells has not been reported.

In the present study, experiments were undertaken to characterize: (1) the relatedness of phages 41c and SPP1; (2) the lytic cycle of phage 41c at the ultrastructural level; and (3) the role of the mesosome during phage 41c infection, or the effect of virus infection on mesosome ultrastructure.

II. REVIEW OF THE LITERATURE

Bacteriophages of Bacillus subtilis

The most recent review article (26) on the bacteriophages of Bacillus subtilis separated the virulent phages into 7 groups. These groupings were based on physical and biological characteristics. For example, phages SP01, SP82G, Ø25, and SP8 were all rather large, virulent phages containing hydroxymethyluracil (HMU) but no thymine in their DNA. Consequently, Hemphill and Whiteley (26) classified them into Group 1 of B. subtilis bacteriophages.

Phage 41c

The B. subtilis phage 41c was isolated from soil by Zsigray et al., 1973 (93). Although the primary goal of that study was to document the sensitivity of phage 41c infection to deoxyribonuclease, it also included results of a partial characterization of the virus. The virus possessed an icosahedral head and a non-contractile tail. The guanine plus cytosine (G+C) content of its double-stranded deoxyribonucleic acid (DNA) was the same (43 mol%) as that of its host, B. subtilis strain 168. Zsigray et al. (93) also found phage 41c to be unique in that its plaquing efficiency decreased by about 98% in agar containing 200 µg/ml of deoxyribonuclease (DNase). They showed that phage development was blocked in 90% of infected cells with the enzyme present during adsorption, whereas the enzyme had little effect 10 min after adsorption. The authors concluded that DNase blocked injection of phage DNA into

the host cell.

Phage 41c has also been shown to be unusual in its ionic requirements. Landry and Zsigray (41) presented evidence for a multi-stage Ca^{++} requirement during infection by 41c. Ca^{++} was specifically required during each of three distinct stages: adsorption, penetration, and intracellular phage development. This differed from the divalent cation ion requirement reported for SF6, a structurally related phage of B. subtilis (80).

Since the adsorption of 41c to the host cell wall had a specific requirement for Ca^{++}, Landry and Zsigray (41) suggested that the ion acts to alter a host or phage receptor site, rather than to neutralize an electrical charge. The role of Ca^{++} in facilitating penetration is less understood. The ion may serve to increase the permeability of the cell membrane to DNA (41). Since these workers demonstrated that neither intracellular transcription nor translation of virus coat proteins was inhibited in the absence of Ca^{++}, the role of this metal during intracellular development of 41c is even less understood.

Phage SPP1

The isolation and characterization of the B. subtilis phage SPP1 has been described (64). The phage possessed a morphology identical to that reported for phage 41c (93). Phage SPP1 DNA had a molecular weight of 2.5×10^7 daltons and a moles % G+C ratio of 43 (64). No unusual bases were indicated. Hemphill and Whiteley (26) assigned phage SPP1 to Group 5 of the B. subtilis phages. It is currently the sole member of this group.

Infection of a B. subtilis 168 culture with phage SPP1 resulted in a latent period of 60 min, followed by an eventual burst size of 200 phage per cell (38). Transfection studies indicated that DNA replication terminated 35 min after initiation of infection. At that time, each cell contained an average of one phage particle (38).

Development of phage SPP1 depended strongly on host functions (16). The presence of a portion of the bacterial RNA polymerase was necessary at all times for phage production (47). Host RNA synthesis continued throughout infection, but it was not determined whether this was necessary for phage replication. Normal expression of host proteins was needed for phage replication (17). SPP1 also required host DNA polymerase III for its replication, although the enzyme was probably modified to some extent during phage infection (49).

There has been considerable interest in the transfection and general transduction properties of phage SPP1 (30,42,76,89). Apparently, phage SPP1 is a good subject for fine structured genetic analyses because its DNA is rapidly denatured into easily separable strands (64). Separation of the denatured DNA results in light and heavy strands, with densities of 1.713 and 1.725 g cm^{-3}, respectively. The buoyant density of intact SPP1 DNA is 1.703 g cm^{-3}. The ease of strand separation is complimented by a high efficiency of strand renaturation (64).

Restriction studies involving phage SPP1 DNA revealed that the maturation of phage SPP1 was imprecise. The individual molecules of phage DNA varied from each other by more than 200 base pairs

even though complete, terminally redundant genomes were produced (30). Nevertheless, both the molecular and the ultrastructural details of the SPP1 maturation process remain obscure.

Ultrastructure of Phage Infections

Gram-negative Bacteria

The ultrastructural changes which occur in host cells during replication and assembly of the T-phages in Gram-negative organisms, especially Escherichia coli, have been studied extensively. A relatively complex pathway for assembly of the T4 head has been described recently (71). Head assembly in this system began on the inner surface of the cytoplasmic membrane (5,75), leading to the formation of membrane-bound prehead structures called T-particles (5,75,36). The T-particles in the T4 system were cleaved from the membrane early in the assembly process. This gave rise to E-particles which are believed to be empty, unexpanded capsids (12). Empty T4 heads were noted both on membranes and in the cytoplasm of E. coli during early maturation of the phage (75).

The detailed replication and assembly mechanisms of several double-stranded DNA phages have been studied in addition to those of the T-phages. Fuller and King (21) examined the problem of self-regulated assembly and control of protein polymerization in the morphogenesis of the Salmonella phage P22. Several ultrastructural studies of filamentous phage infections have also been described (7,53,72). The majority of these studies reported the formation of intracellular membranes in the infected host cells.

Bradley and Dewar (7) reported that the infective process of filamentous phages stimulated the production of excess cell wall and cell membrane materials in E. coli. They speculated that this strengthened the envelope during the extrusion of virions, since filamentous phage infections usually did not result in lysis and death of the host cells. Instead, particles were extruded continuously over a period of time. The formation of membranes appeared 20-30 min prior to the appearance of filamentous particles. Similar observations were made with the filamentous phages f1 (72) and fd (53). The appearance of membranous structures in fd-infected E. coli cells was linked specifically to incomplete phage maturation at the cell membrane, rather than solely to the inhibition of host cell growth or to infection with mutant phage. Schwartz and Zinder (72) proposed that completed f1 particles either pass directly through or are assembled on the cell membrane.

Gram-positive Bacteria

In contrast to the numerous studies on phage-infected Gram-negative cells cited above, relatively few such studies have been reported for Gram-positive cells. Phage infections of Bacillus cells have been examined at the ultrastructural level, but most of these reports are either brief or somewhat superficial. Tikhoneko and Bespalova (81) reported that the formation of phage N1 particles occurred in the nuclear vacuole of B. mycoides, and that phage particle maturation did not occur synchronously. Similar results were noted in studies of B. thuringiensis cells infected by the phage I-97 (3). The first change noted in the infected cells was an enlargement of the nuclear region. This was followed by the

appearance of phage-like,electron-dense particles in the nuclear region of the cells. Tails were not detected. Similar structural changes have been reported to occur in cells of Clostridium perfringens infected with the short-tailed phage 80 (8). In this case, the nuclear region enlarged and became dispersed. Mature phage particles were formed, and lysis resulted from degradation of the cell envelope.

A relatively detailed ultrastructural study of B. subtilis infected with phage AR7 (2) indicated that empty-headed phage particles occurred frequently in the infected cells. These particles were usually seen in the ribosomal part of the cytoplasm, while full heads were generally located in the nuclear region. Although vesicular-type mesosomes (intracellular membranes) were observed in the uninfected cells, the authors did not notice any alteration, disappearance, or increase in frequency of these structures during infection.

A study of Ø29 morphogenesis in B. subtilis (52) has identified three classes of particles during phage maturation. These included proheads, empty heads, and mature phage. The authors did not feel that the empty heads were true intermediates in the assembly process, because they were observed only in thin-sections of cells that had been restrictively infected with sus (suppressor-sensitive) mutants. By comparison, ultrastructural studies of lytic infection by phage Ø25 in B. subtilis (43) also revealed the presence of empty-headed particles. Liljemark and Anderson (43), however, felt that these unfilled capsids may have been precursors to filled capsids in the packaging process of this phage. They further characterized the

intracellular development of phage Ø25 by correlating the ultrastructural studies with the kinetics of host and phage DNA synthesis. Although this description of intracellular phage development in B. subtilis was quite extensive and well documented, it did not mention the appearance of mesosomes. These structures were visible in several of their micrographs, however, and it appeared that these structural characteristics were not affected by the phage infection.

Mycoplasma Cells

Phylogenetic studies indicate that the mycoplasmas arose as a degenerate subline from the Gram-positive bacteria (85). Therefore, it seemed reasonable to examine the morphology of virus replication in these microorganisms. Ultrastructural studies of Acholeplasma laidlawii infected with MVL3 virus revealed that assembly and maturation of the virus involved cell membrane processes (25). Infection of this organism culminated in the release of infectious particles without the loss of cell viability (45). Infected cells synthesized and released MVL3 particles for hours. Adsorption of this double-stranded DNA virus to the mycoplasma was characterized by a clustering or capping on the cell membrane (25). Electron micrographs also showed progeny virus aligned on the membrane, with their tails oriented toward its cytoplasmic surface. Some infected cells had membrane invaginations between groups of membrane-associated MVL3 particles. Frequently, singular extracellular virions were observed enclosed within small membrane vesicles. The authors indicated that, since centrifugation was a part of their preparative procedure, these vesicles must still have been attached to the host cell. Larger vesicles were also found within cells. These con-

tained many viruses with their tails towards the membrane, and may have been formed by evaginations of infected cells. Nevertheless, no data were obtained in regard to how such membrane vesicles formed or how they released the MVL3 particles.

Ultrastructure of Mesosomes

Mesosomes, or invaginations of the cytoplasmic membrane to form intracellular membranous structures (18), have been observed frequently in Gram-positive bacteria (24). Mesosomes have occasionally been reported to occur in E. coli cells (35,59,67), but Greenawalt and Whiteside (24) suggested that the term be restricted to structures characterized as: (i) intracellular membranes which are clearly the result of an invagination of the plasma membrane (i.e., they include a "neck" or "stalk") forming a pocket or sac containing membranous components and (ii) the components within sacs become extruded upon cell plasmolysis, or removal of the cell wall. In only one case, have structures fitting this description been found in Gram-negative cells (66).

In recent years, the in vivo configuration of mesosomes has been a rather controversial subject. The substructure of mesosomes, as well as their location within the cell, may depend on the fixation procedure employed for cell preservation (10,11,20,22,27,51,73). The substructure was usually described as either tubular, vesicular, or lamellar in these studies.

The effects of fixation by OsO_4 on the formation or preservation of mesosomes has never been clarified. Numerous investigators prepared bacterial samples by a variety of techniques which were

designed to preserve mesosomes in their true form. However the results were quite inconsistent. Fooke-Achterrath, et al. (20) felt that chilling of samples prior to fixation provided "closer-to-life" preservation of the mesosomes. They concluded that true mesosomes were small and peripherally located, as opposed to the artifactual, centrally located, larger mesosomal bodies. Ghosh and Nanninga (22) described two types of mesosomes, peripheral and cytoplasmic. The former seemed to be unaffected by the fixation. Results of their studies also indicated that different organisms reacted differently to similar fixation procedures.

The presence of mesosomes in freeze-etched or negatively-stained cell preparations has also proven to be a controversial subject. It was reported that mesosomes required fixation in order to be observed in frozen-etched (27), or negatively-stained samples (28). Burdett and Rogers (11) claimed that large mesosomes were consistently formed at the poles and at the septal regions of negatively-stained cells. These mesosomes were similar in size to those detected in thin sections.

The ionic composition of the fixation buffer has also been shown to play a role in determining the ultrastructure of mesosomes. Burdett and Rogers (10,11) found that the mesosomes appeared lamellar in configuration when the buffer solution had either a low ionic strength or a low concentration of divalent cations. Low sucrose concentrations produced a mixture of vesicular and lamellar type mesosomes, while higher concentrations produced the vesicular type only (10). Since buffers and salts accelerated the fixation and provided osmotic stability, they concluded that

the majority of mesosomes were filled with vesicular and tubular membranous material (as opposed to the lamellar type) in normal, rapidly growing cells (10). In contrast to this, Silva (73) found that the omission of calcium and uranyl ions in the Ryter-Kellenberger fixation (37) led to the almost complete disappearance of the mesosomes.

Results of a more sophisticated study (57) suggested that mesosomes were formed when localized sites on the cell membrane were pulled from close contact with the cell wall into the cytoplasm. The action of a fixative or other physiological disturbance on a cytoplasmic component, such as DNA, was shown to have such an effect on Streptococcus faecalis cells.

Additional studies on mesosome ultrastructure have indicated that centrifugation (27), thermal injury (74), and composition of external gases (58) could affect the appearance of mesosomes. A recent report has gone so far as to claim that classical mesosomes were nothing more than artifacts of the preparative techniques involved (15).

III. MATERIALS AND METHODS

General Procedures

Phage and Bacterial Strains

The isolation of phage 41c has been described (93). A stock lysate was supplied by R.M. Zsigray (Department of Microbiology, University of New Hampshire). Phage SPP1 was obtained from D.M. Ellis (The Bacillus Genetic Stock Center, The Ohio State University). A stock lysate of phage SP82G was a gift from D.M. Green (Department of Biochemistry, University of New Hampshire).

Bacillus subtilis 168 trp^- str^r (93) was the predominant bacterial strain used throughout this study.

Media

Liquid media employed for the growth of the host cells and for infection studies were TYS (93) and TP (34) broths. TYS medium consisted of the following ingredients per liter of distilled water: tryptone, 10 g; NaCl, 10 g; yeast extract, 5 g. TP medium consisted of the following ingredients per liter of distilled water (pH 7.0): glucose, 2 g; tris-hydrochloride (pH 7.0), 2.4 g; maleic acid, 2.3 g; $(NH_4)_2SO_4$, 1 g; NaCl, 5 g; K_2HPO_4, 0.1 g; acid-hydrolyzed casein (salt-free, vitamin-free), 0.2 g; tryptophan, 0.02 g; $MgCl_2 \cdot 6H_2O$, 4 g; $MnCl_2 \cdot 4H_2O$, 0.02 g; $FeCl_3 \cdot 6H_2O$, 2.7 mg.

Solid media contained the same ingredients as TYS and TP broths with the addition of 1.5% or 0.85% agar (Difco, Detroit, MI) for basal media and for soft agar overlays, respectively.

For optimal growth of phages 41c and SPP1, all media were supplemented with 10 mM $CaCl_2$ (41). Both 10 mM $CaCl_2$ and 10 mM $MgCl_2$ were added to media used for phage SP82G lysate preparations, experiments, and titrations.

Preparation of Spore Stock

Lab-Lemco agar (Oxoid, London, England) plates streaked with an exponentially growing (in TYS broth) culture of B. subtilis 168 were incubated for 3-4 days at 37°C. Spores and freshly grown cells were then washed from the surface of the agar with 3-4 ml of sterile saline. The suspensions were washed twice in sterile saline and heat treated at 70°C for 20 min to kill vegetative cells. Resulting spore suspensions were stored in sterile, screw-capped, glass culture tubes at 4°C.

Phage Enumeration

Phage titrations were determined by a modification of the soft agar overlay method described by Adams (1). Serial dilutions of the phage were made and 0.1 ml of the appropriate dilution was inoculated onto the basal medium. Approximately 4 ml of the desired overlay, seeded with host cells, was added to the plated sample and mixed by gentle swirling in a "figure-8" rotation. Solidified plates were inverted and incubated 18-24 h at 37°C, after which the number of plaque-forming units per ml (PFU/ml) was determined.

Preparation of Phage Lysates

B. subtilis 168 cultures (1 liter) were grown to an optical density (OD) of 0.5 at 670 nm in 2.8-l Fernbach flasks at 37°C on a

rotary shaker at 350 rpm. Cultures were then infected with phage at a multiplicity of infection (MOI) equal to 5. Aeration and incubation at 30°C was continued for 3-5 h. The lysate was stored at 4°C overnight and then cleared of intact cells and cellular debris by centrifugation at 15,000 x g for 10 min. Extraneous and/or host nucleic acids were degraded by the subsequent incubation of the lysate at 37°C for 1 h in the presence of 10 µg/ml each of deoxyribonuclease I (DNase I, Worthington Biochemicals, Freehold, N.J.) and ribonuclease A (RNase A, Worthington).

The phage lysates were filter sterilized through a 0.45-µm Millipore filter (Millipore Corp., Bedford, Ma.). When necessary, the lysates were concentrated by ultracentrifugation at 80,000 x g for 2 h. The bluish, mucoid pellets (sedimented phage) were combined following resuspension in physiological saline.

Phage Characterization Studies

Determination of Morphological Characteristics

For negative staining, concentrated phage lysates were placed on parlodion-coated, carbon-reinforced, 400-mesh, copper specimen grids and mixed with 1% phosphotungstic acid (pH 7.2). The excess liquid was drawn off the grid surface, and the phage preparations were allowed to air dry. Samples were immediately viewed and photographed with a JEOL JEM-100S transmission electron microscope operating at an accelerating potential of 80 kV. Phage dimensions were reported as the average of at least 20 measurements determined from the electron micrographs with an ocular micrometer.

Host Ranges of Phages 41c and SPP1

Twelve TYS soft agar overlays were prepared in 50-ml volumes. Each of these was seeded with one of the Bacillus strains listed in Table 1. Petri dishes containing TYS basal medium were then inoculated with 0.1 ml of either phage 41c or SPP1. These plates were then inoculated with 4 ml of the appropriate seeded overlay. Each overlay was also added to 2 TYS plates lacking phage. All plates were incubated at 37°C except for those containing B. megatherium. These were kept at 30°C. After 24-48 h of incubation, the plates were examined for confluent growth of the prospective host and areas of clearing or lysis by the phage.

Sensitivity of Infection to Deoxyribonuclease

Phages 41c and SPP1 were tested for their sensitivity of infection to the nuclease, deoxyribonuclease I (93). The DNase sensitivity was determined in TYS broth to which 200 µg/ml DNase and 10 mM $MgCl_2$ was added prior to phage infection. Samples were assayed for phage enumeration following a 15-min incubation period at room temperature (26°C).

Effect of Streptomycin on the Efficiency of Plaquing

The effect of streptomycin on the efficiency of plaquing for phages 41c and SPP1 was determined on TYS basal medium supplemented with 1 mg/ml of streptomycin sulfate (Eli Lilly and Co., Indianopolis, IN). The same concentration of streptomycin sulfate was added to the soft agar overlays as well. The PFU/ml which were obtained with this assay were directly compared to those obtained in the absence of the antibiotic.

TABLE 1

Bacterial strains

Bacterium	Source*
B. subtilis 168	U.N.H. stocks (I. Miller)
B. subtilis 6633	American Type Culture Collection
B. subtilis B-6	U.N.H. stocks (J. Rake)
B. subtilis QMB 1228	U.N.H. stocks (A. Bernheimer, W.R. Chesbro)
B. subtilis QMB 1228(supra)	U.N.H. stocks (L. Ardisson)
B. subtilis W-23	O.E. Landman, Georgetown University
B. licheniformis 749/c	U.N.H. stocks
B. megatherium	U.N.H. stocks
B. pumilus	U.N.H. stocks
B. cereus	U.N.H. stocks
B. mycoides	U.N.H. stocks

*Individuals responsible for deposition of bacterium into U.N.H. (University of New Hampshire) stock collections are given in parentheses.

Determination of Velocity Constants (K Values) of Antiserum

Rabbit antiserum to phage 41c was a gift from R.M. Zsigray (Department of Microbiology, University of New Hampshire). The velocity constants (K values) of the antiserum (diluted 1:100) against phages 41c and SPP1 were determined by the method of Adams (1). A 5-min interval was allowed for interaction of phage and antibody. Assays were done in triplicate and the experiment was repeated twice.

Determination of Molecular Weights of Phage Structural Proteins

Lysates of phages 41c and SPP1 were prepared and concentrated by ultracentrifugation and lyophilization. Protein concentrations were determined spectrophotometrically with a Bausch and Lomb Spectronic-20 using a protein-dye binding method (6). The proteins were disrupted by heating the samples to 100°C for 2 min in the presence of 2-mercaptoethanol and 0.1% sodium dodecyl sulfate (39). Separation of proteins was accomplished by polyacrylamide gel electrophoresis as described by Ornstein (55) and Davis (14), with the addition of 0.1% SDS. Optimum results were obtained with 10% polyacrylamide slab gels, 35-40 µg protein per well, and a constant current of 16 mAmps. The protein bands were visualized following fixation and staining at 37°C (overnight) with 0.1% Coomassie Brilliant Blue R-250 (Mann Research Lab., New York, NY) dissolved in 50% trichloroacetic acid. Gels were destained in 10% acetic acid. The molecular weights of the protein subunits were determined from a standard curve (84) based on the migrations of the following standards: phosphorylase b (94,000 daltons), bovine

serum albumin (67,000 daltons), ovalbumin (43,000 daltons), carbonic anhydrase (30,000 daltons), and soybean trypsin inhibitor (20,000 daltons). All standards were obtained from Pharmacia Fine Chemicals, Piscataway, N.J.

Determination of Phage DNA Base Composition

Extraction of phage DNA. Concentrated phage lysates were purified using a preformed CsCl gradient as described by E.F. Landry (40). A CsCl stock was prepared by dissolving 20 g of CsCl in 13.2 ml of distilled water and 1.5 ml of 0.01 M Tris (pH 7.0). Seven substocks were prepared by adding 1.7 ml, 1.6 ml, 1.5 ml, 1.4 ml, 1.3 ml, 1.2 ml, and 1.0 ml of CsCl stock to 7 tubes and adjusting the final volume to 2.0 ml with Tris buffer. The gradient was prepared by adding, in descending concentration, 0.5 ml of CsCl substocks. One and one-half ml of the concentrated virus was layered on the gradient and centrifuged at 73,400 x g (R_{av}) for 30 min at 4°C in a swinging bucket rotor. The cellulose nitrate tube was tapped and the dense blue band was collected.

The phage DNA was extracted by the addition of 5 ml of saline sodium-citrate (SSC) saturated phenol (44) to an equal volume of a concentrated phage lysate. The sample was gently agitated at 4°C for 30 min and centrifuged at 12,000 x g for 10 min. The supernatant was collected using an inverted 10-ml pipette and added to an equal volume of SSC-phenol. The extraction was repeated 2-3 times for 20 min at 4°C. The supernatant fluid from the final extraction was dialyzed against 1 liter of SSC (pH 8.0)

at 4°C with changes at 1, 3, and 5 h, followed by dialysis overnight. The DNA was collected and stored at 4°C. DNA concentrations were determined spectrophotometrically at 260 nm with a Beckman DU-8 spectrophotometer.

Chromatographic Analysis. DNA extracted from phage 41c was hydrolyzed with formic acid as described by Wyatt and Cohen (87), or by the enzymatic action of DNase I in the presence of $MgCl_2$ followed by treatment with snake venom phosphodiesterase (Worthington) for 6 h (60). Enzymatic treatment of the DNA was conducted at 37°C. DNA from concentrated suspensions of phage SPP1 was also hydrolyzed enzymatically. Following hydrolysis, the samples were concentrated by evaporation overnight at 37°C in a vacuum oven, and resuspended in a small volume of 0.1 N HCl. The individual nucleotides were separated by descending paper chromatography using Schleicher and Schull no. 2043a paper and an isopropanol: HCl:water solvent (86). Hydrolyzed phage DNA, hydrolyzed calf thymus DNA, and appropriate standards were spotted in duplicate. Standards included thymine, adenine, cytosine, guanine, and uracil for comparison with chemical hydrolysates. Their phosphorylated derivatives (e.g. UMP, TMP) were used for comparison with enzymatically hydrolyzed samples. Approximately 30 µg of standard DNA bases and 100-120 µg of hydrolyzed DNA were chromatographed in each case. The solvent was allowed to descend either 15-20 or 35-40 cm. Chromatograms were then air dried and immediately observed with short-wave ultraviolet light.

Preparation of 41c and SPP1 DNA labelled with ^{3}H-thymidine.

Twenty ml of B. subtilis 168 trp$^-$ thy$^-$ mutant was grown in TP broth to an OD of 0.5, centrifuged at 12,000 x g for 5 min and resuspended in 20 ml of fresh TP broth containing 5 µg/ml thymidine. Approximately 2 µCi/ml of ^{3}H-thymidine (New England Nuclear, Boston, MA) was added and aeration was continued for 5 min at 37°C. The culture was equally divided into 2 small flasks and infected with either phage 41c or SPP1 at a MOI of 10. The mixtures were incubated at 30°C with aeration for 2-4 h. The lysates were centrifuged and the supernatant fluids were treated with DNase I in the presence of $MgCl_2$ and RNase A (final concentration = 10 µg/ml each) for 1 h at 37°C. The labelled phage were filtered through a 0.45-µm Millipore filter and concentrated by ultracentrifugation. The supernatant was decanted and the pellet was washed by resuspension in saline followed by another 2 h of ultracentrifugation. The washed sample was finally resuspended in 10 ml of fresh TP broth. The labelled phage were assayed for PFU/ml and counted for radioactivity as described below.

A small aliquot of labelled phage (0.2 ml) was added to scintillation vials containing 10 ml of Aquasol-2 (New England Nuclear). The vials were inverted several times and counted for radioactivity in a Beckman LS-7000 automatic scintillation counter. Counts were corrected for background and the CPM/PFU were determined for both labelled phage.

Nuclear magnetic resonance spectroscopy of phage 41C DNA.

Approximately 1-1.5 mg of DNA extracted from a concentrated lysate of phage 41c was enzymatically hydrolyzed as described above.

After evaporation of the liquid (SSC), the dried nucleotides were resuspended in a small volume (1-2ml) of D_2O (Aldrich Chemical Co., Metuchen, N.J.) and the spectrum of proton shifts was determined with a JEOL FX900 NMR Spectrometer. Since thymidine was the nucleotide of interest; a spectrum for pure thymidine dissolved in D_2O was also determined. Sodium 3-trimethyl-silypropane sulfonate (Sigma Chemical Company, St. Louis, MO) was used as a reference for all spectra. Data interpretations were made by K. Gallagher (Instrumentation Center, University of New Hampshire).

Plaquing Efficiency of Phages 41c and SPP1

Since 10 mM Ca^{++} is required for efficient plaquing by phage 41c (41), it was necessary to determine if phage SPP1 had the same Ca^{++} requirement. Stock lysates of both phages were diluted and assayed for PFU/ml in TYS medium, both in the presence and absence of added Ca^{++}.

Mixed Infections with Phages 41c and SPP1

A culture of B. subtilis 168 was grown to an OD of 0.5 and simultaneously infected with phages 41c and SPP1. The MOI for each phage was 0.5. At 4 h post-infection, the lysate was assayed for PFU/ml and the plates were incubated at 37°C for 18 h. The total PFU/ml for each of the phage was determined based on easily discernable differences in their plaque morphology.

Physiological Studies

Burst Curve for Phage 41c

At 15 min following initiation of infection (MOI=25), 0.5 ml of a 41c-infected culture was removed and an equal volume of rabbit antiphage 41c serum (neutralization constant = 30) was added. Subsequent to incubation for 10 min at 30°C, the sample was diluted in TYS broth and maintained on the shaker at 30°C. Subsamples were assayed for PFU/ml for the next 120 min.

Phage 41c-Directed Protein Synthesis

To determine the approximate time of completion for phage 41c-directed protein synthesis, a culture of B. subtilis 168 was infected with phage 41c at an MOI of 10. An appropriate period of time (15 min) was allowed for adsorption of phage and penetration of DNA. Subsequently, 2 ml of the infected culture was distributed into each of 12 screw-capped test tubes. At 20 min post-infection, chloramphenicol (CAP; Parke, Davis, and Co., Detroit, MI) was added to one of these tubes at a final concentration of 20 µg/ml. CAP was added to each of the remaining tubes at 5 min intervals for the next 50 min. A control tube was left untreated. All tubes were aerated with a Wrist Action Shaker (Burrell) at room temperature for approximately 180 min post infection. Final ODs were then determined on a Bausch and Lomb Spectronic-20 colorimeter at a wavelength of 670 nm.

Host DNA Synthesis During Infection with Phages 41c and SPP1

The incorporation of ^{3}H-thymidine into B. subtilis 168 thy^{-} trp^{-} cells grown in TP medium (34) containing 10 mM Ca^{++} was monitored during infection with phage 41c or SPP1. The cell growth on a TP plate that had been incubated overnight at 37°C was suspended in saline and used to inoculate 30 ml of TP broth (supplemented with 20 µg/ml each of thymidine and tryptophane) to an OD of 0.05. The culture was incubated at 37°C and agitated at 350 rpm until the OD reached 0.5. The cells were then rapidly sedimented by centrifugation and resuspended in 30 ml of fresh TP broth containing 1 mg/ml $CaCl_2$, 5 µg/ml thymidine, and 2 µCi/ml of ^{3}H-thymidine (New England Nuclear). These cells were then incubated at 30°C with rapid agitation for 5 min. The culture was split into three 10-ml volumes and a sample aliquot (0.2 ml) was removed from each (preinfection samples). One of the three 10-ml cultures was infected with phage 41c and another with phage SPP1. The MOI in each case was 10. Samples were periodically removed from each culture for up to 115 min post-infection. Samples were diluted in 10% trichloroacetic acid, stored on ice, and filtered through Millipore membranes (0.45-µm) as described by Liljemark and Anderson (43). Dried filters were added to liquid scintillation vials containing 10 ml of cocktail (Aquasol-2; New England Nuclear) and counted for 10 min on a Beckman LS-7000 automatic liquid scintillation counter.

To further verify the continuity of host replication, the OD of an uninfected culture as well as that of a 41c-infected culture were monitored on a Spectronic-20 throughout the lytic cycle. TYS

broth containing $CaCl_2$ was utilized for these spectophotometric studies.

Electron Microscopical Studies

Preparation Techniques

Fixations. Whole cells were prepared for transmission electron microscopy either by the Ryter-Kellenberger technique (37) or by the Fooke-Achterrath procedure (20). For the Ryter-Kellenberger process, cells were prefixed by adding 1% OsO_4 (in Kellenberger buffer) to the culture medium to bring the final OsO_4 concentration to 0.2%. Cells were then concentrated by centrifugation, washed in Kellenberger buffer, suspended in tryptone-salt solution (1% tryptone, 0.5% NaCl), and embedded in 2% Noble agar (Difco). The agar was cut into small blocks, which were postfixed for 18 h in 1% OsO_4 (in Kellenberger buffer) and prestained for 3 h in 0.5% uranyl acetate (in Kellenberger buffer), prior to dehydration and embedding as described below.

For the Fooke-Achterrath fixation, the samples were chilled rapidly by submerging the plastic centrifuge tube containing them in liquid nitrogen for 25 s. The tubes were swirled continuously to prevent freezing of the cells. Samples were then prefixed, postfixed, and prestained as in the Ryter-Kellenberger technique (above), except that the prefixation was carried out at $4^{\circ}C$.

Protoplasts (see below) were prepared for electron microscopy by adding 10 ml of sample to a centrifuge tube containing aqueous glutaraldehyde. The final concentration of the fixative was 1.25%. These were kept at $4^{\circ}C$ for 20 min, centrifuged at 12,000 x g for

15 min, and resuspended in 2% Noble agar (Difco). All samples were postfixed with 1% OsO_4 in Kellenberger buffer overnight, stained, dehydrated, and infiltrated as described for whole cells.

Thin sectioning. Samples from all fixation procedures were dehydrated through a graded ethanol series and embedded in Spurr's low-viscosity epoxy resin (78). Sections were cut with glass knives on an LKB Ultratome III ultramicrotome, using a cutting speed of 2 mm/s and a clearance angle of 2-3°. Sections were retrieved with uncoated 400-mesh, copper grids. They were then poststained for 15 min with 0.5% uranyl acetate (in 50% methanol) and for 1 min with 0.4% lead citrate (62).

Transmission electron microscopy. Samples for transmission electron microscopy were viewed and recorded with a JEOL, JEM 100S electron microscope at an accelerating potential of 80 kV. At least 30 cell sections were photographed for each sample. These were analyzed for mesosome configuration, presence of viral structures, nature of the nucleoplasm, and general appearance of the cytoplasm.

Effects of Fixation on Ultrastructure of Mesosomes

An uninfected culture was grown to an OD of 0.5 and a variety of fixation procedures were employed on separate portions of the sample. A prefixation with OsO_4 was applied at final concentrations of 0.1%, 0.2%, 0.5%, and 1%. In addition, prefixations with OsO_4 at a final concentration of 0.2% or 1% were done on cells which were either subjected to centrifugation or to chilling at

-195°C (see above).

Cells which had been prefixed with 2.5% glutaraldehyde before and after centrifugation were also examined. All subsequent post-fixations, dehydrations, infiltrations, and sectioning of samples were done as described above.

Studies on the Infection Cycle in Whole Cells

A TYS broth culture was shaken at 37°C until it reached an OD of 0.8. The culture was then diluted with TYS broth to an OD of 0.5. One liter of this diluted culture was transferred to a shaker operating at 350 rpm at 30°C, and samples (10 ml) were withdrawn for electron microscopy. The culture was then infected with either 41c, SPP1, or SP82G at a MOI of about 25. Samples were withdrawn for electron microscopy immediately, 15 min, and 30 min after initiation of infection. Thereafter, samples were withdrawn at 5-min intervals through 85-min post-infection. For each time period during phage 41c infection, one of two duplicate samples withdrawn was prepared for thin sectioning by the Ryter-Kellenberger technique (37), and the other was processed by the Fooke-Achterrath procedure (20). For each time period during infection with SPP1 or SP82G, a single sample was processed for thin sectioning by the Ryter-Kellenberger technique only.

Elemental Analyses of Whole Cells

Both uninfected and infected cultures were analyzed by energy-dispersive X-ray analysis (EDAX). A B. subtilis 168 culture was grown to an OD of 0.5 in TYS broth containing $CaCl_2$. The culture

was separated into 3 portions. One portion was infected with phage 41c, another with phage SPP1, and the third portion was left untreated. Following aeration and incubation at 30°C for 40 min, each of the cultures was concentrated by centrifugation and resuspended in 2 ml of 10 mM $CaCl_2$. The samples were immediately frozen in ethanol and lyophilized. The powdered samples were then subjected to elemental analysis using an EDAX system coupled to an AMR 1000 scanning electron microscope, operating at 20 kV. In all cases, 20,000 counts were collected. Results were interpreted on the basis of percent detectable elements.

Studies on the Infection Cycle in Whole Cells Treated with CAP

Phage 41c-infected cells (MOI=20), treated with CAP (20 µg/ml) at 20 min post-infection were also prepared for viewing by transmission electron microscopy. The infected cells were incubated at 37°C with aeration for an additional 40 min following treatment with the antibiotic. The samples were then prepared for microscopy by the Ryter-Kellenberger fixation procedure (37), as described above.

Studies with Protoplasts

Protoplast formation. Protoplasts were prepared as previously described (93). Acid-washed glassware was used for all protoplast work. Cells were grown in TYS broth to an OD of 0.2, concentrated, and resuspended in one-fourth the original volume of TYS. Lysozyme (Sigma) was added to the culture at a final concentration of 400 µg/ml. At the same time a stock solution of 2 M sucrose or 2 M

sorbitol was added to the culture to bring the final concentration of the sugar to 0.5 M. The lysozyme-treated samples were incubated at 30°C with gentle agitation (25 rpm) until protoplast formation was complete. This was monitored by phase-contrast microscopy with a Zeiss standard research microscope.

Protoplast stability. To determine the effectiveness of sucrose and sorbitol in stabilizing protoplasts, 600 ml of B. subtilis 168 was grown to an OD of 0.2 in TYS broth. The cells were concentrated by centrifugation and resuspended in 150 ml of fresh TYS. The culture was then split into 2 equal volumes. One portion received 25 ml of 2 M sucrose, the other received 25 ml of 2 M sorbitol. The final concentration of the stabilizer in both cases was 0.5 M. Each of these was then treated with lysozyme and gently agitated for the remainder of the experiment. The OD was periodically recorded with a Bausch and Lomb Spectronic-20. In addition, direct counts were made using a Zeiss phase-contrast microscope and a Petroff-Hauser bacteriological counting chamber.

Experiments with protoplasts were also designed to assess the lytic properties of various diluents and assay procedures. Cells were grown in TYS as described above, and infected with phage 41c at a MOI of 1. Aeration and incubation at 37°C was continued for 15 min and a portion was removed and assayed for PFU/ml. The culture was then treated with CAP (20 μg/ml) in the presence of sucrose. After 45 min, the culture was divided into 4 parts. Each of the parts was then assayed for PFU/ml by one of the following methods: (i) diluent, basal medium and overlay were composed of TYS and 0.5 M sucrose, (ii) saline was used for the diluent and

TYS for basal medium and overlay (without sucrose), (iii) diluent, basal medium and overlay were composed of TYS (without sucrose), (iv) same as (iii) except that 0.1 ml of chloroform was added to the first tube of the dilution blanks to insure lysis of the protoplasts. $CaCl_2$ was added to all diluents, overlays, and basal media.

Replication of phage 41c in protoplasts. Cells were grown in TYS broth and infected with phage 41c as described above. After 15 min of aeration and incubation at 30°C, 0.4 ml of antisera to phage 41c (K=3) was added to 15 ml of culture. The infected cells were immediately assayed for PFU/ml. The remaining culture material was treated with CAP and lysozyme as described above. At the same time, 5 ml of 2 M sucrose or sorbitol was added to the culture to bring the final concentration of the stabilizer to 0.5 M. The mixtures were then incubated at 30°C with very slow agitation (25 rpm). When protoplast formation was greater than 99% completed, the culture was diluted 100-fold in TYS containing 0.5 M stabilizer. Subsamples were then periodically removed and assayed for PFU/ml.

Each of the subsamples were assayed in TYS medium with and without 0.5 M sucrose. When sucrose was omitted from the dilution broth, basal medium, and agar overlay, then 0.1 ml of chloroform was added to the first tube of the diluent. All the media were supplemented with $CaCl_2$. The PFU/ml was determined from the plates after 18 h of incubation at 30°C.

Preparation of protoplasts from phage 41c-infected cells.

B. subtilis 168 cells grown to an OD of 0.2 in TYS broth (500 ml) were centrifuged and resuspended in TYS broth as described above. Phage 41c was added to yield a MOI of 40. After 25 min of aeration and incubation at 30°C, 0.3 ml of antisera to phage 41c (K=30) was added to the culture. Subsamples (9 ml) were removed at 15, 30, 40, 50, 60, and 75 min post-infection and added to 50-ml flasks containing 5 ml of 2 M sucrose, 0.5 mg CAP, and 8 mg lysozyme. When protoplast formation was complete, 10 ml of each of these samples was prefixed with aqueous glutaraldehyde and prepared for transmission electron microscopy as described above.

IV. RESULTS

Phage Characterization Studies

Size and Morphology of Phages 41c and SPP1

Electron micrographs of negatively stained phage 41c (Figure 1a) indicated that the head possessed an icosahedral structure and was approximately 60 nm in diameter. The flexible tail was quite visible, but tail fibers, base plates, and contractile sheaths were not detected. The neck appendage or collar, which was apparent in empty-headed phage, measured 15-20 μm across. The morphology of phage SPP1 (Figure 1b) was essentially identical to that of phage 41c. The dimensions of each phage are listed in Table 2.

Host Range and Plaque Morphology

Of the 11 strains listed in Table 1, only Bacillus subtilis 168 supported the replication of phage 41c or SPP1. In addition, six mutants of B. subtilis 168 which were isolated as a result of spontaneous resistance to infection by phage 41c proved to be resistant to phage SPP1 infection as well.

After 24 h of incubation at 37°C, the plaques produced by phage 41c were small (approximately 2 mm in diameter) and circular in shape. Each plaque had a clear center, surrounded by a pronounced translucent halo. Phage SPP1 produced circular areas of

FIGURE 1

Electron micrographs of phage negatively stained with 1% phosphotungstic acid (pH 7.2). Bars = 0.25 μm.(A), phage 41c; (B), phage SPP1.

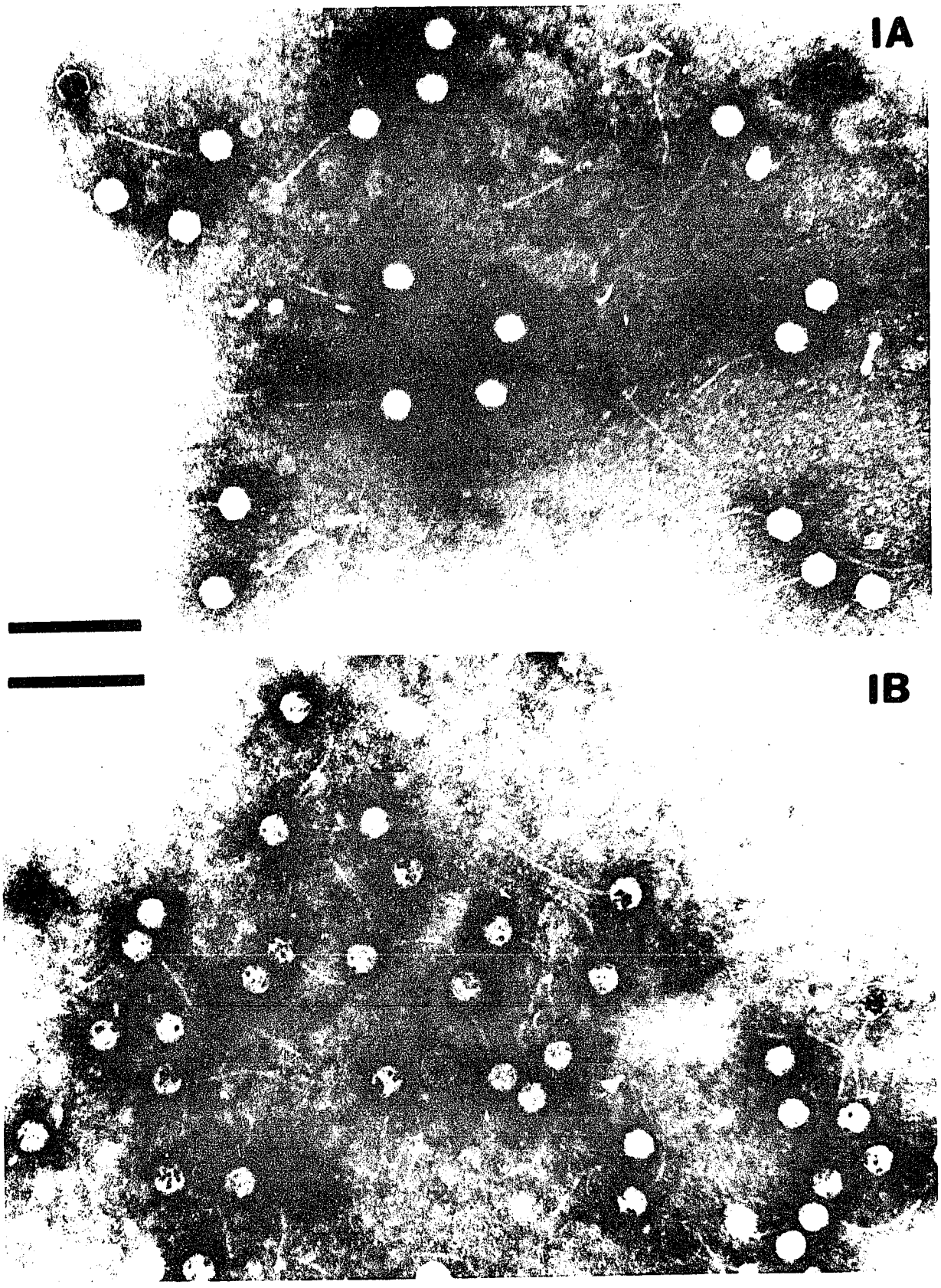
IA
IB

TABLE 2

Dimensions of phages 41c and SPP1

Phage	Dimensions (nm)		
	Head Diameter	Tail Length	Tail Width
41c	59±3	194±10	10±2
SPP1	61±2	182±5	9±1

clearing (3-4 mm in diameter). A faint halo was infrequently visible at the periphery of the plaque.

Inhibition of Infection by Deoxyribonuclease or Streptomycin

Infection by either phage 41c or SPP1 was significantly inhibited by the presence of either DNase (Table 3) or streptomycin (Table 4). In the latter case, any plaques that did appear were pinpoint in size and transparent for both phages.

K Values of Antisera and Molecular Weights of Phage Structural Proteins

The K values (neutralization constants) for rabbit antisera to phage 41c were 50 and 25 for phages 41c and SPPI, respectively. As these results might predict, only slight differences were detected between the molecular weights of the structural protein subunits of the two phages. Results of polyacrylamide gel electrophoresis (PAGE) indicated a minimum of 15 distinct protein subunits from heat-disrupted lysates of phages 41c or SPP1 (Figure 2). The high density of the migrating protein front suggested the presence of additional protein subunits. However, these proteins were not separated due to the technical limitations of the electrophoretic system available. Nevertheless, the gel pattern produced by phage 41c clearly resolved a 54,000 dalton protein subunit which was not detected in the SPP1 gel pattern. Similarly, lysates of SPP1 revealed a protein subunit with a molecular weight of approximately 41,500 daltons which was not detected in lysates of 41c. All other bands were similar, but not always identical, in molecular weight.

TABLE 3

Phage recovery in the presence of deoxyribonuclease

Phage	DNase concentration (μg/ml)	PFU/ml*	Recovery (%)
41c	-	3.7×10^7	-
41c	200	7.2×10^5	1.9
SPP1	-	2.5×10^7	-
SPP1	200	3.1×10^5	1.2

*Data indicates the average of plaque assays done in triplicate.

TABLE 4

Recovery of phage in the presence of streptomycin sulfate

Phage	Streptomycin Concentration (mg/ml)	PFU/ml*	Recovery (%)
41c	-	6.6×10^{10}	-
41c	1	1.4×10^{10}	17
SPP1	-	5.8×10^{10}	-
SPP1	1	1.4×10^{10}	19

*Data indicates the average of plaque assays done in triplicate.

FIGURE 2

SDS-polyacrylamide slab gel containing structural proteins of phages SPP1 and 41c. Each well contained 35-40 µg of protein. Position of standard bands are indicated on righthand side of figure. (a), SPPI proteins; (b), 41c proteins.

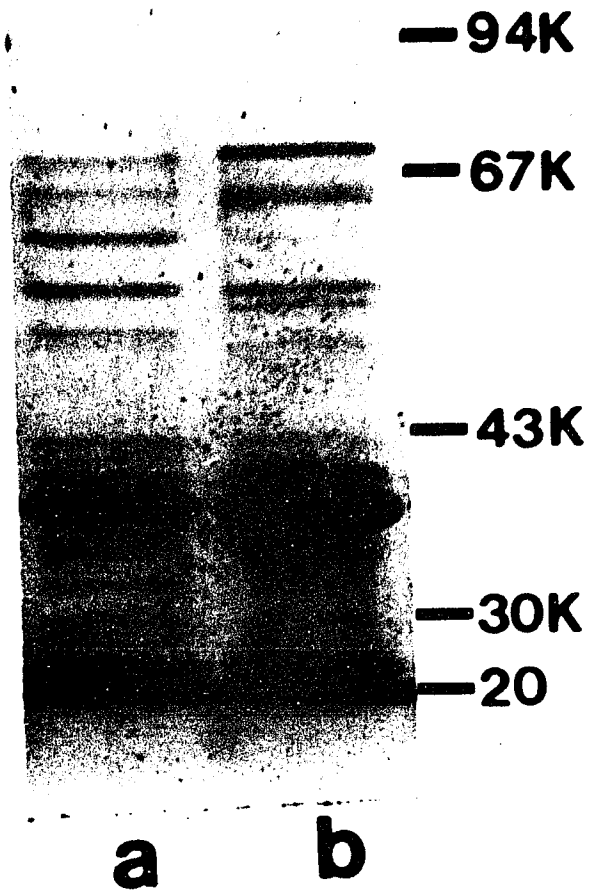
94K
67K
43K
30K
20
a
b

The molecular weights of the phage proteins, as determined from these gel patterns, are listed in Table 5.

Base Composition of Phages 41c and SPP1 DNAs

Results of thermal denaturation and CsCl buoyant density ultracentrifugation of phage 41c DNA suggested that no unusual bases were present (93). However, these methods could not discriminate between "normal" DNA (possessing thymine) and DNA containing the pyrimidine uracil in place of thymine. Therefore, several other methods were utilized to demonstrate the presence of thymine in 41c DNA. These included chromatographic analysis, ^{3}H-thymidine uptake experiments, as well as nuclear magnetic resonance (NMR) spectroscopy.

Chromatograms of formic-acid hydrolyzed 41c DNA yielded R_f values of approximately 0.26, 0.35, and 0.43. A fourth spot was faintly visible and was calculated to have an R_f value of 0.68. These values most likely represented the bases guanine, adenine, cytosine, and uracil, respectively. They matched the R_f values of the standards used in this study, which in turn, were almost identical to those reported previously (33,86). In addition, chromatograms of enzymatically digested 41c DNA revealed a spot with an R_f value of 0.62. This was identical to that obtained with the UMP standard. Furthermore, a spot with an R_f value determined to be representative of thymidine was detected in chromatographs of hydrolyzed SPP1 DNA.

Although the chromatography data suggested that 41c DNA possessed uracil and SPP1 DNA contained thymine, a phage 41c

TABLE 5

Approximate molecular weights (in daltons) of protein subunits for phages 41c and SPP1

Phage 41c	Phage SPP1
120,000	120,000
70,000	70,000
66,000	66,000
60,000	62,000
55,000	56,000
54,000	52,000
49,000	43,000
43,000	41,500
40,000	40,000
36,500	38,000
34,000	36,000
33,000	33,000
30,500	30,500
28,500	28,500

lysate produced in the presence of ^{3}H-thymidine produced 6 x 10^{9} PFU/ml and contained 49,400 CPM/ml. A similar experiment with phage SPP1 resulted in a lysate containing 1 x 10^{10} PFU/ml and 59,900 CPM/ml. Therefore, phage 41c and phage SPP1 lysates produced by identical means possessed 8 x 10^{-6} CPM/PFU and 6 x 10^{-6} CPM/PFU, respectively.

The presence of thymine in phage 41c DNA was finally confirmed by NMR spectroscopy (Table 6). Enzymatically hydrolyzed DNA (resuspended in D_2O) readily produced a peak at 1.92 ppm. A peak at this position is characteristic of a methyl group such as that which occurs on the pyrimidine thymine (K. Gallagher, personal communication). None of the other bases (adenine, cytosine, guanine, or uracil) possess such methyl groups. Due to the relatively low concentration of phage 41c DNA used, many of the other peaks characteristic of thymidine were not apparent.

Plaquing Efficiency of Phages 41c and SPP1

The data in Table 7 indicated that the efficiency of plaquing (EOP) for both phages 41c and SPP1 was inhibited by a factor of about 90% in the absence of Ca^{++}. However, when Ca^{++} was omitted from TYS broth the resulting lysates of either phage showed more than a 99.9% decrease in PFU. The latter phenomenon was evident even when these lysates were assayed in the presence of Ca^{++}. Furthermore, intact phage were not detected in negatively stained preparations of the presumed lysates. These results, which are in agreement with those of Landry and Zsigray (41), suggest that Ca^{++} is required for a post-penetration step

TABLE 6

Nuclear magnetic resonance spectroscopy

Spectral Peak Assignments (in parts per million)			
Literature Values*		Experimental Data**	
thymidine	uridine	thymidine	Phage 41c DNA
1.91	3.72	1.9	1.92
2.4	3.7	2.38	2.68
3.79	4.87	3.8	2.75
3.85	5.63	3.99	2.77
4.03	5.85	4.48	4.26
4.49	7.89	6.29	5.33
6.28	10.99	7.65	7.93
7.65	-	-	8.54
-	-	-	8.67

*(References 4,68).

**Both pure thymidine and phage 41c DNA (hydrolyzed) was dissolved in D_2O and subjected to nuclear magnetic resonance spectroscopy of the proton shifts.

TABLE 7

Effect of calcium (10 mM) on the efficiency of plaquing for phages 41c and SPP1

Experiment Number	Phage	Calcium Added (mM)	PFU/ml*	Inhibition (%)
1	41c	10	6.4×10^{10}	-
	41c	0	6.3×10^{9}	90.1
	SPP1	10	7.6×10^{10}	-
	SPP1	0	7.3×10^{9}	90.4
2	41c	10	1.4×10^{10}	-
	41c	0	2.2×10^{9}	84.2
	SPP1	10	1.3×10^{10}	-
	SPP1	0	1.2×10^{9}	90.6
3	41c	10	1.7×10^{10}	-
	41c	0	2.2×10^{9}	86.8
	SPP1	10	1.2×10^{10}	-
	SPP1	0	1.1×10^{9}	91.1

*Data indicates results of plaque assays done in triplicate.

in the production of phage 41c. The results of this study also show that such a requirement applies to the production of phage SPP1 progeny.

Mixed Infection with Phages 41c and SPP1

Simultaneous infection of B. subtilis 168 with phages 41c and SPP1 resulted in a normal burst size of about 10^3 phage per cell. As evidenced from their distinctively different plaque morphology, phages 41c and SPP1 did not exclude each other from infecting the host cells (Table 8). Approximately 50% of the plaques were typical of those produced by phage 41c. All others were characteristic of phage SPP1.

Physiological Studies

Characterization of the Lytic Cycle by Enumeration of Phage Progeny

Quantitative data on the appearance of viral progeny after infection of Bacillus subtilis with phage 41c are given in Figure 3. Infection was followed by a latent period of approximately 50 min. The number of free phage rose exponentially for about 120 min, resulting in a burst size of approximately 10^3 phage per host cell.

Phage 41c-Directed Protein Synthesis

The data presented in Figure 4 indicate that the addition of chloramphenicol at 30 min after infection protected more than 75% of the infected complexes from lysis. Since CAP is a potent inhibitor of protein synthesis, these data indicate the presence of

TABLE 8

Simultaneous infection of B. subtilis 168 with phages 41c and SPP1*

Experiment Number	Final PFU/ml**	
	Phage 41c	Phage SPP1
1	3.7×10^{10}	4.8×10^{10}
2	3.3×10^{10}	2.6×10^{10}
3	2.0×10^{10}	3.2×10^{10}

*The input in all three experiments was adjusted to 1.2×10^{8} PFU/ml for each of the phage.

**The final PFU/ml is the average of the plaque assays done in triplicate per experiment.

FIGURE 3

Intracellular growth curve of phage 41c. Arrows indicate times after infection when samples were withdrawn for electron microscopy.

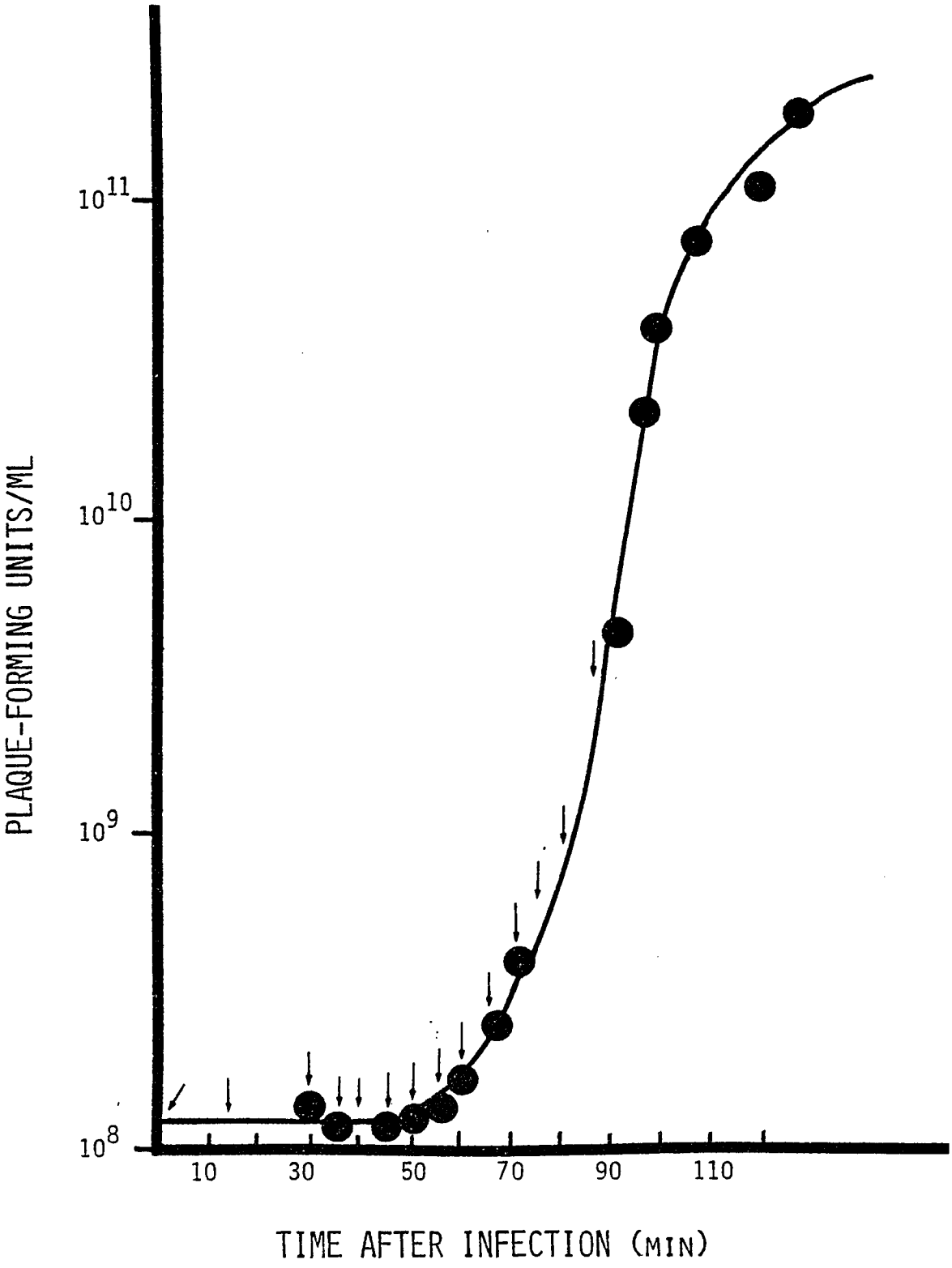
PLAQUE-FORMING UNITS/ML
10^{11}
10^{10}
10^{9}
10^{8}
10
30
50
70
90
110
TIME AFTER INFECTION (MIN)

FIGURE 4

Effect of chloramphenicol on the optical density of B. subtilis cultures infected with phage 41c. Following infection, a culture was divided into twelve portions. At 5 min intervals, (from 20-60 min post-infection), one of the subcultures was treated with chloramphenicol (20 µg/ml). Samples were aerated and incubated for approximately 3 h post-infection, before the final optical density values were determined.

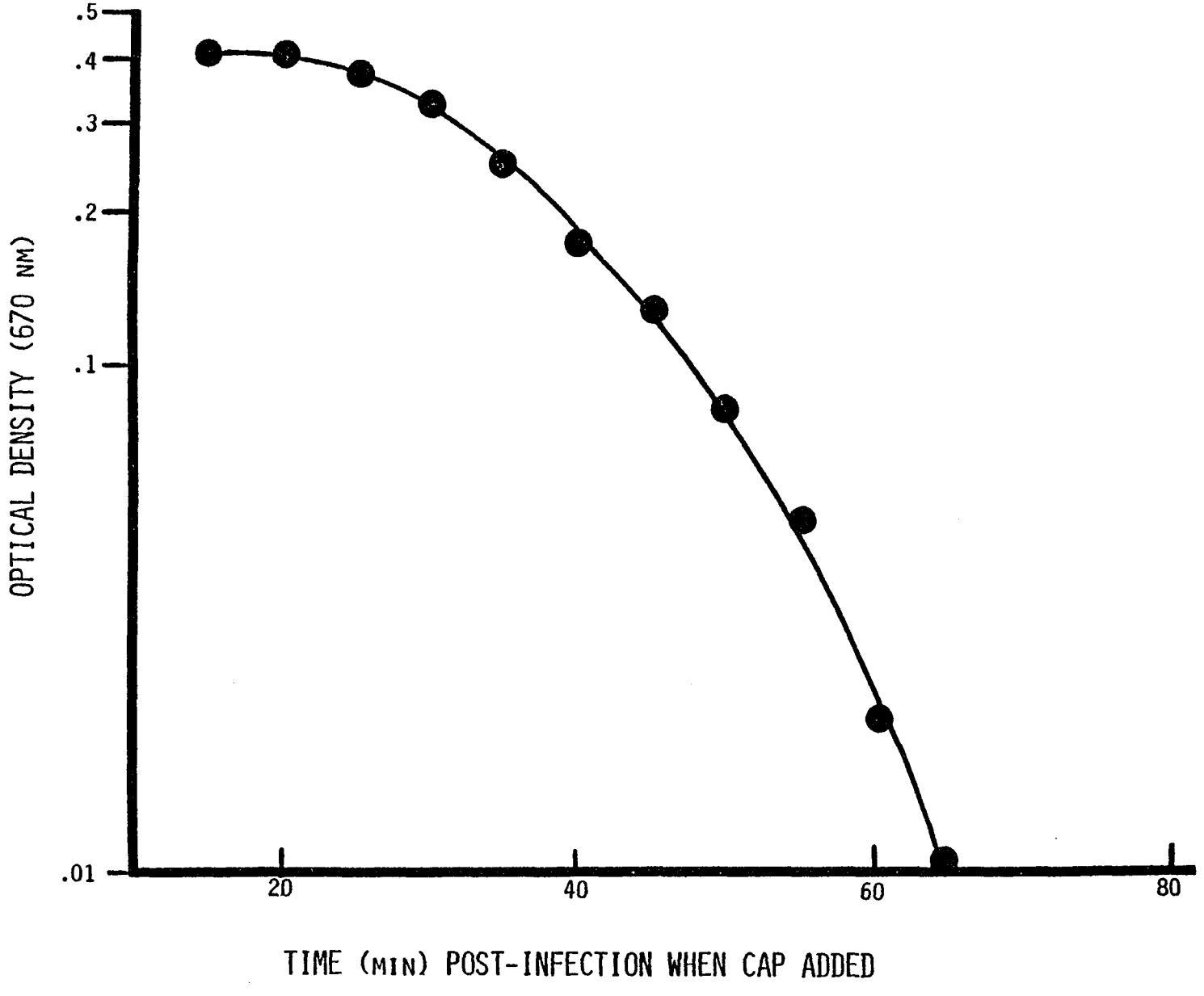
.5
.4
.3
.2
.1
.01
OPTICAL DENSITY (670 NM)
20
40
60
80
TIME (MIN) POST-INFECTION WHEN CAP ADDED

sufficient phage proteins to allow assembly and some lysis of the culture. Since an MOI of about 10 was used, an infected culture without CAP lysed within 120 min post-infection.

Host DNA Synthesis During Infection with Phages 41c and SPP1

Studies by Esche (16) have established that infection by phage SPP1 does not inhibit host DNA synthesis. In this study, B. subtilis cells infected with phage 41c incorporated ^{3}H-thymidine at the same rate as did those infected with phage SPP1 (Figure 5). Thus, it appeared probable that 41c infection also failed to significantly alter host DNA synthesis. Furthermore, the OD of a B. subtilis culture infected with phage 41c increased at the same rate as that of an uninfected culture until the onset of lysis (Figure 6), suggesting a normal growth pattern for cells during early stages of infection.

Electron Microscopical Studies

Ultrastructure of Uninfected Cells

Uninfected cells preserved by the Ryter-Kellenberger procedure (37; Figure 7) were similar in ultrastructure to exponentially growing B. subtilis cells that have been described previously (51, 82,83). The nucleoplasm in most of these cells was concentrated in one or more discrete, centrally located regions. Thin, electron-dense strands were often visible within these regions. The cytoplasm appeared as a granular electron-dense area. Individual ribosomes were usually not delineated clearly. Most longitudinal

FIGURE 5

Uptake of ^{3}H-thymidine by B. subtilis grown in TP broth. Symbols: ●, uninfected culture; ■, culture infected with phage 41c; □, culture infected with phage SPP1.

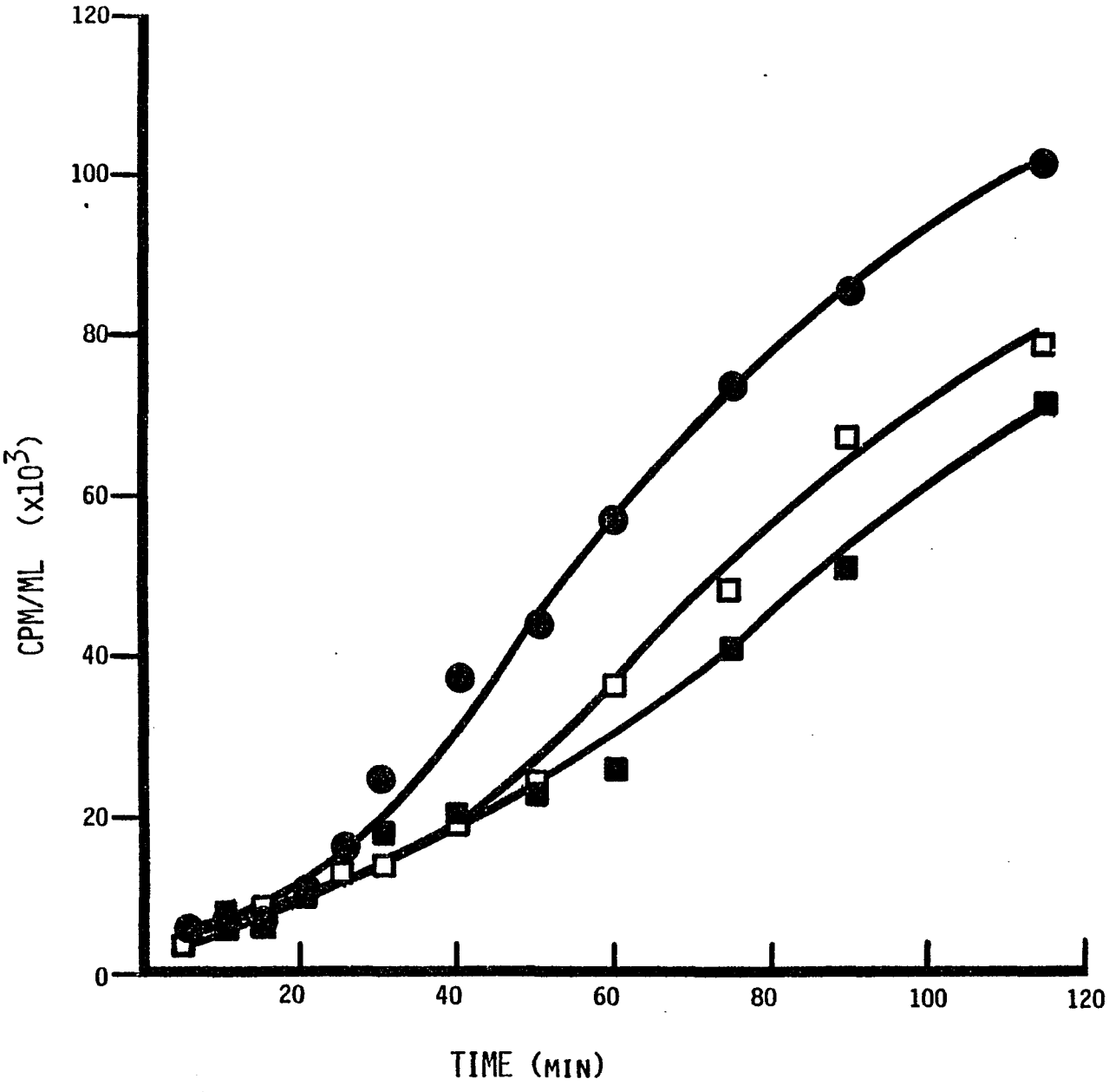
120
100
80
60
40
20
0
CPM/ML (x10^3)
20
40
60
80
100
120
TIME (MIN)

FIGURE 6

Effect of phage 41c infection on host replication. Symbols: ● , uninfected culture; ■ , culture infected with phage 41c as indicated by arrow.

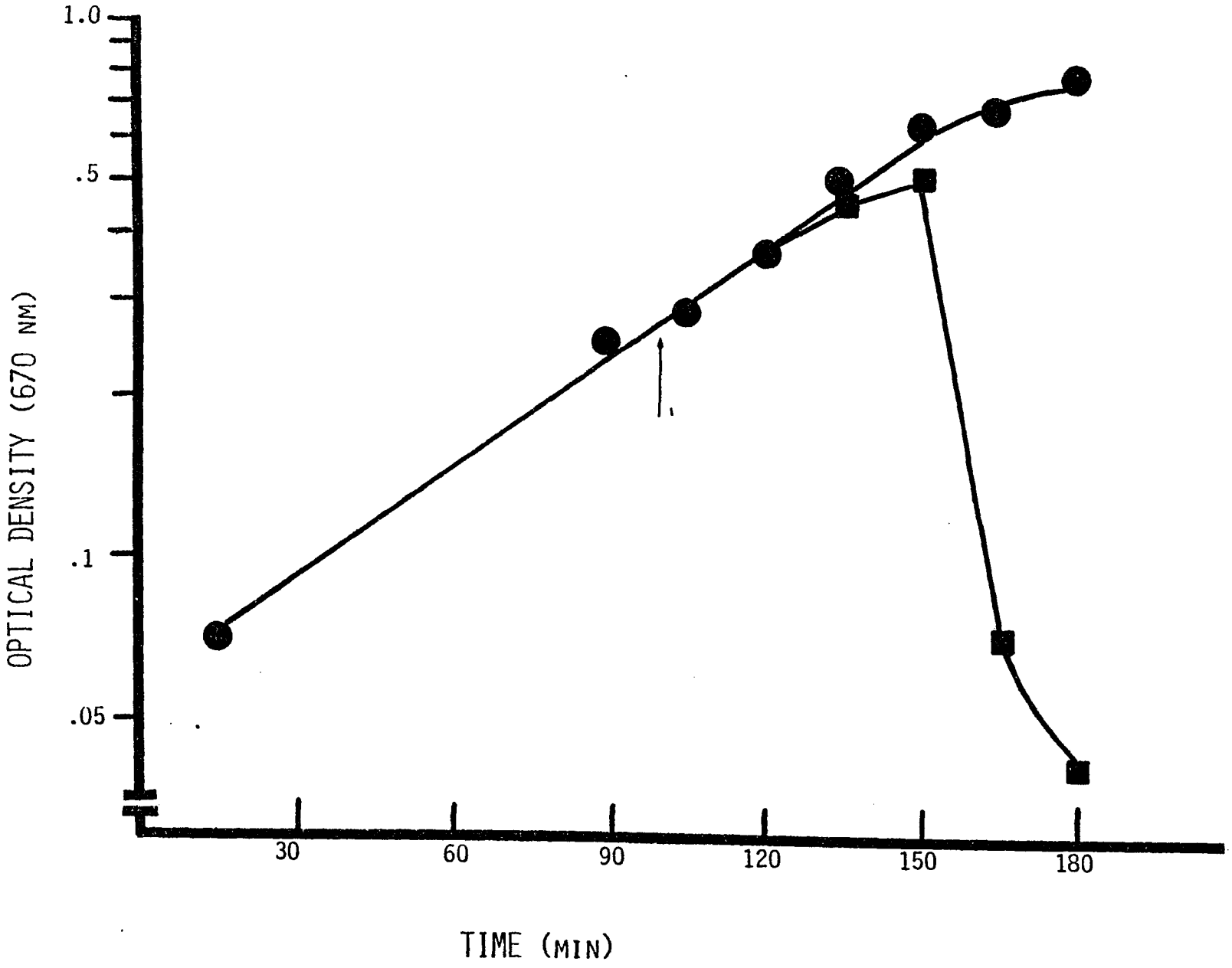
1.0
.5
.1
.05
OPTICAL DENSITY (670 NM)
30
60
90
120
150
180
TIME (MIN)

FIGURE 7

Electron micrograph of thin-sectioned, uninfected B. subtilis cell (Ryter-Kellenberger fixation). Longitudinal section, showing discrete, centrally located nucleoplasm (n) and a tightly packed, vesicular-lamellar mesosome (m). Bar = 0.5 μm.

FIGURE 8

Electron micrograph of thin-sectioned, uninfected B. subtilis cell showing mesosome structure (Ryter-Kellenberger fixation). Detail of typical, centrally located, tightly packed, vesicular mesosome (m). Note association with division septum. Bar = 0.3 μm.

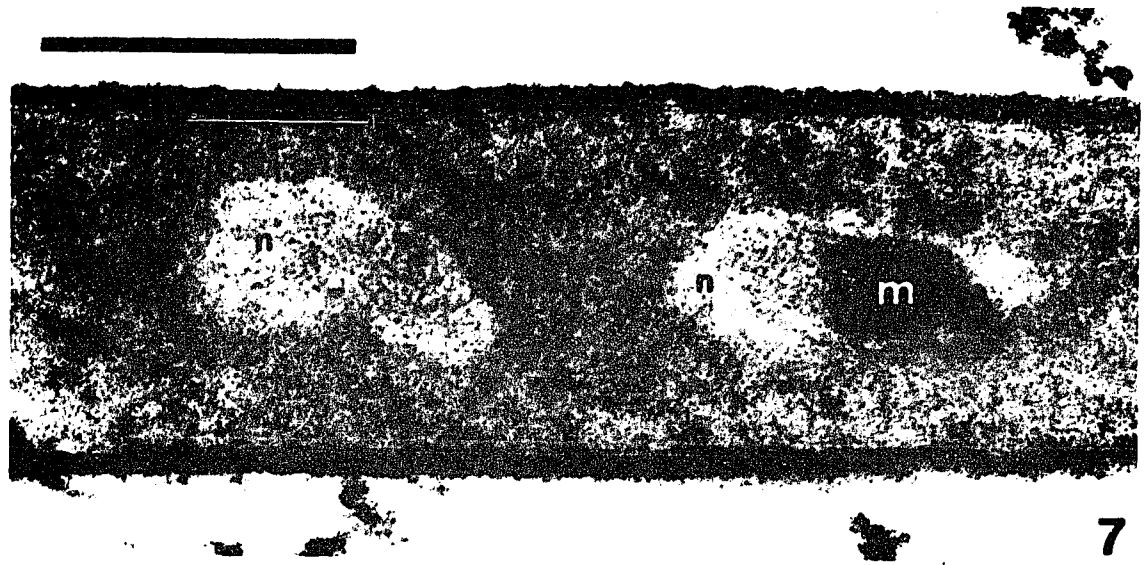

7

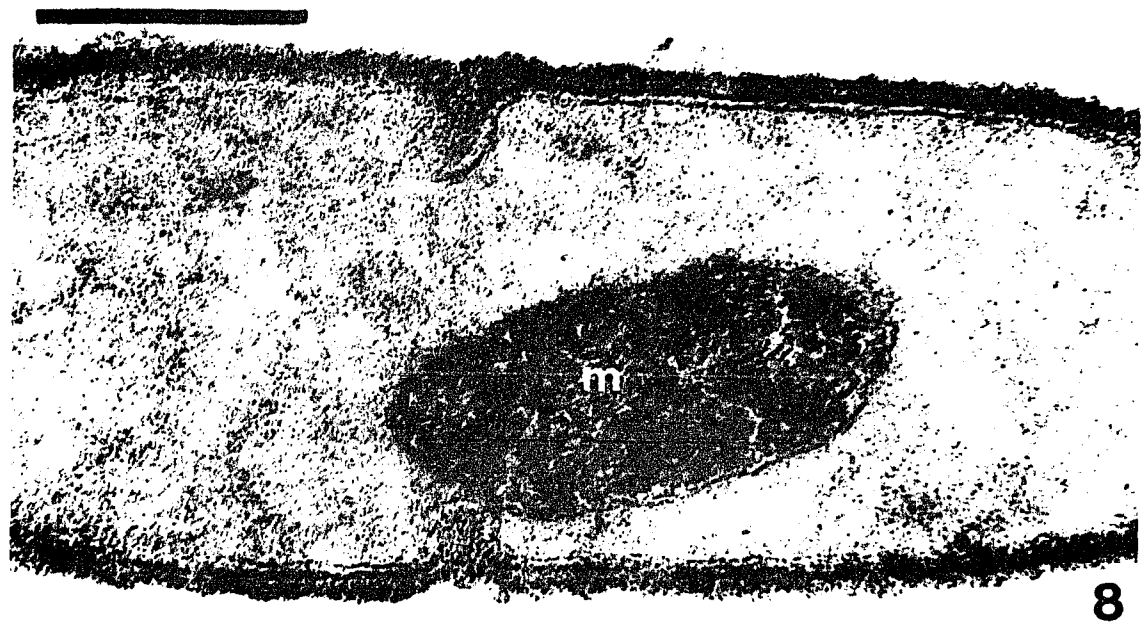

8

sections contained one or more large, complex mesosomes in addition to the usual nuclear and cytoplasmic materials. The main bodies of these mesosomes were often centrally located with respect to the short axis of the cell. They ranged in diameter from 0.08 to 0.4 μm, with an average diameter of 0.22±0.07μm. The arrangement of their internal components was often vesicular and, sometimes, vesicular-lamellar (24). Fully lamellar mesosomes were relatively rare. The internal membranes of almost all mesosomes were ordered in a fairly compact, tightly folded configuration. Association of the mesosomes with division septa were clearly visible in some cell sections (Figure 8), as were connections to the peripheral cytoplasmic membrane. No significant changes were observed in the ultrastructure of uninfected cells throughout the 85-min incubation period. Furthermore, centrifugation of cells prior to prefixation did not alter the ultrastructure of these cells or their mesosomes.

Cells prepared for electron microscopy by the Fooke-Achterrath technique (20) were ultrastructurally similar to those fixed by the Ryter-Kellenberger method (37). However, the location, size, and frequency of their mesosomes differed. The mesosomes were smaller and more peripherally located structures (Figure 9). Although they were observed at approximately three times the frequency as those observed following preparation by the Ryter-Kellenberger method (37), they maintained the vesicular configuration described above.

Cells prefixed with glutaraldehyde generally appeared to be poorly preserved. Mesosomes were rarely seen. When visible,

FIGURE 9

Electron micrograph of thin-sectioned, uninfected B. subtilis cell (Fooke-Achterrath fixation). Longitudinal section, showing discrete, centrally located nucleoplasm (n) and several peripherally located, vesicular or vesicular-lamellar mesosomes (m). B = 0.25 μm.

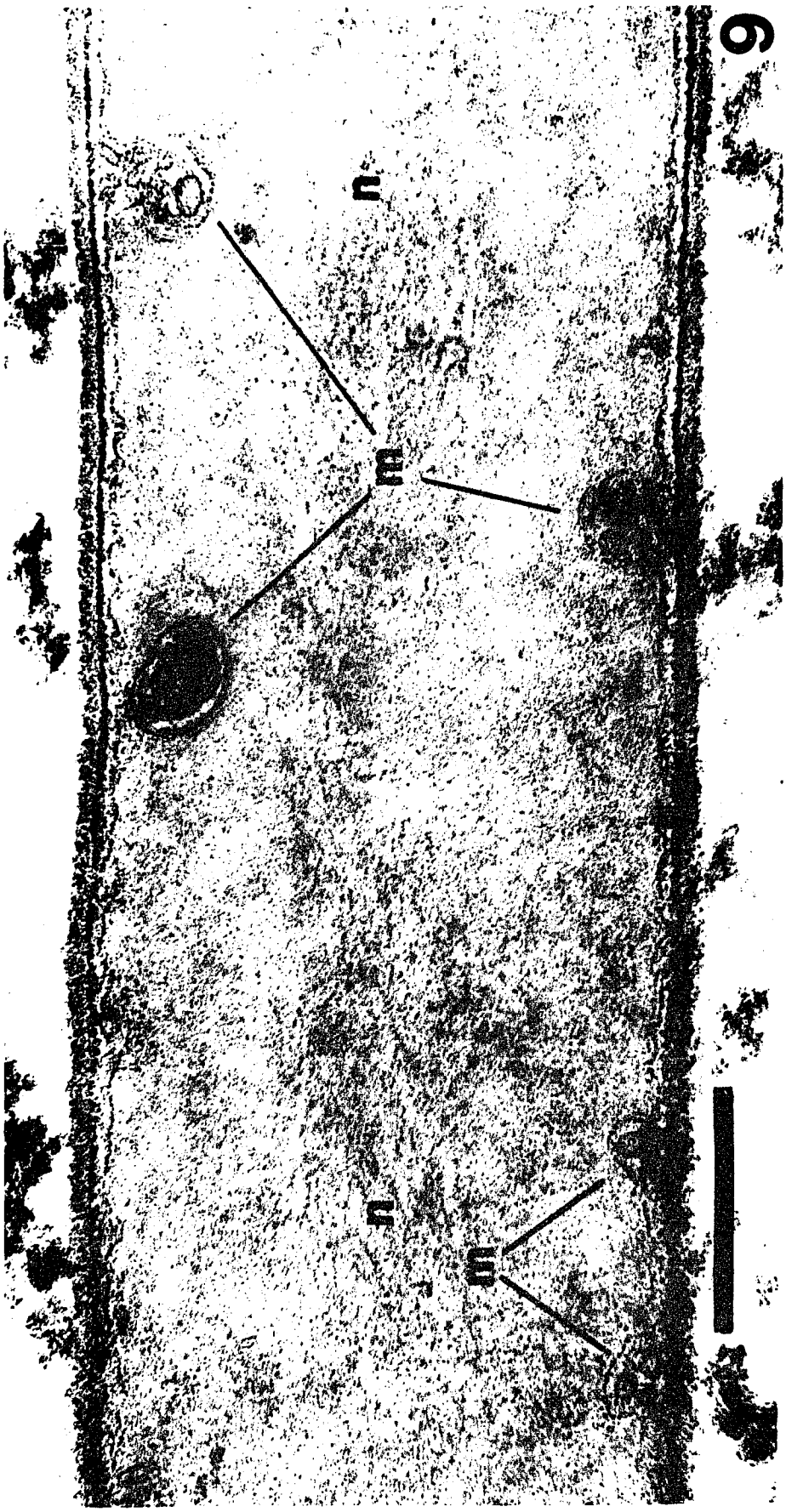
6
n
m
n
m

they appeared to be small, vesicular in configuration, and peripherally located like those seen with the Fooke-Achterrath procedure (20).

Ultrastructure of Cells Infected with Phage 41c

Ryter-Kellenberger fixation. Sampling times for the electron microscopical studies described below extended throughout the latent and well into the burst period as defined by the results in Figure 3. Cells infected with phage 41c either in the presence of added Ca^{++} or added Ca^{++} and Mg^{++}, and preserved with the Ryter-Kellenberger procedure (37) were ultrastructurally identical to control cells fixed by this method (described above) for up to 30 min post-infection. However, morphological changes did take place in the host before any definite viral structures were seen within the cytoplasm. The first of these changes was observed between 35 and 40 min after infection. The mesosomes in some cells began to open up slightly. Their internal membranes were no longer as compact or as tightly packed as they were in uninfected cells.

Considerable changes in the ultrastructural features of infected cells occurred between 40 and 50 min post-infection. Both the extent to which mesosomes were altered and the proportion of cells containing altered mesosomes increased markedly during this period. The mesosomes underwent a transition from the vesicular arrangement seen in uninfected cells (Figure 8) to a lamellar configuration. This transition appeared to start at the outer portions of the mesosomes and then move inward until a fully

lamellar arrangement was formed (Figures 10a and 10b). The mesosomes in 90% of the cell sections observed had taken on the fully lamellar configuration within 50 min following infection. The mesosomes also continued to unfold or open up, sometimes spreading throughout the cytoplasm (Figure 10c), as the above transition took place. The first definite phage structures appeared concurrently with the alteration of the mesosomes. These structures were seen in about 20% of the cells between 40 and 50 min after infection. Many of them appeared to be located in close proximity to or on the surface of the membranes in the altered mesosomes (Figure 11). The cytoplasm of many cells became less electron-dense between 40 and 50 min after infection, presumably due to phage-accumulated DNA. All of these ultrastructural changes occurred between 50 and 70 min after infection which corresponds to the interval between the appearance of phage particles and cell lysis. The proportion of cells containing viral particles increased to 90% during this period. The number of phage heads per longitudinal cell section also increased markedly; as many as 100 were seen in some cases. The phage heads (Figures 12-14) averaged 45 nm in diameter, were electron-dense, and had distinct edges when they were contained entirely within the plane of sectioning. On the other hand, neither phage tails, nor empty heads were ever clearly visible. The phage heads were no longer preferentially associated with the membrane surfaces of the altered mesosomes by this time. They accumulated as clusters throughout the cytoplasm instead, while most of the mesosomes assumed a rather distinctive spiral or concentric configuration (Figure 12). At the same time,

FIGURE 10

Electron micrographs of thin-sectioned cells between 40 and 50 min after infection with phage 41c, showing probable sequence of mesosome alteration (Ryter-Kellenberger fixation). Bars = 0.2 μm. (A) Mesosome still in transition between vesicular and lamellar forms; outer portion is lamellar (l) while inner portion is vesicular (v). (B) Mesosome in fully lamellar configuration. (C) Fully lamellar mesosome that has opened up and spread throughout the cytoplasm.

FIGURE 11

Electron micrographs of thin-sectioned cells between 40 and 50 min after infection with phage 41c, showing association of phage with altered mesosomes (Ryter-Kellenberger fixation). (A) Mesosome that has spread throughout cytoplasm. Phage (p) are arrayed along surfaces of mesosomal membranes. Bar = 0.3 μm. (B) Mesosome is opened, lamellar configuration with phage situated along its outer surface. Bar = 0.1 μm.

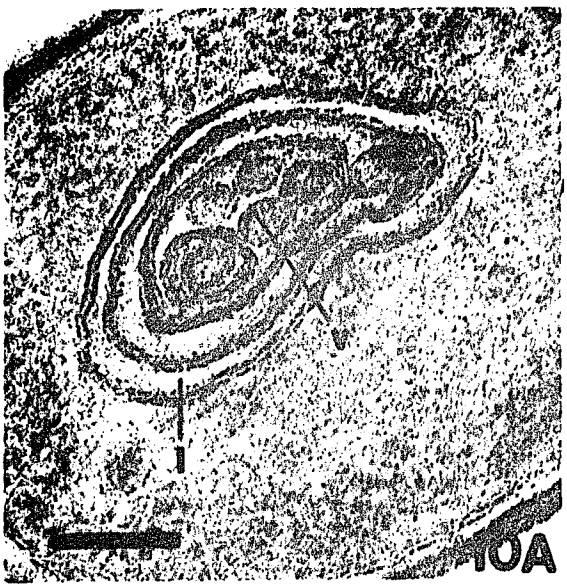

10A

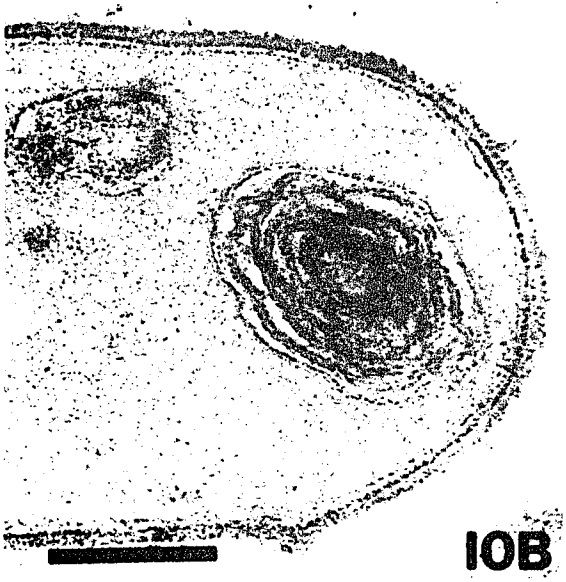

10B

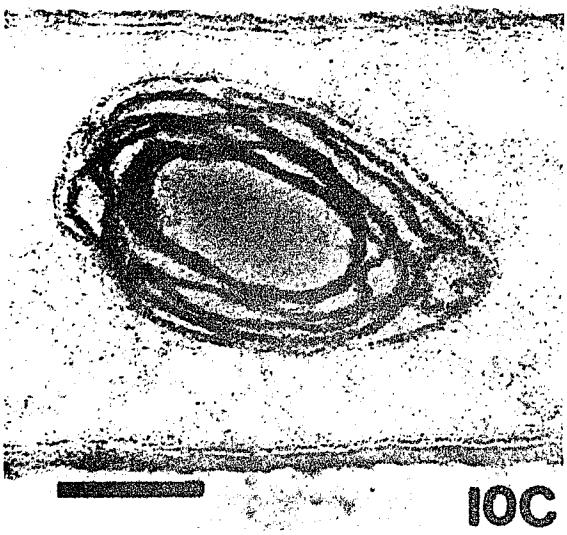

10C

11A

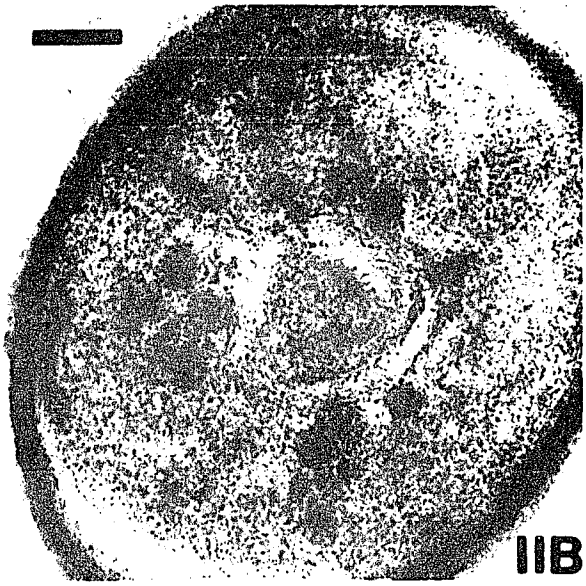

11B

FIGURE 12

Electron micrograph of thin-sectioned cell 65 min after infection with phage 41c (Ryter-Kellenberger fixation). Cytoplasm contains many phage heads, some of which (p) are fully in plane of sectioning and have distinct edges. Note the distinctive spiral or concentric configuration of mesosomes. Bar = 0.25 μm.

FIGURE 13

Electron micrograph of thin-sectioned cell 70 min after infection with phage 41c, showing early stages of lysis (Ryter-Kellenberger fixation). Cell wall has been degraded at several points while cytoplasmic membrane has remained largely intact. Note large mesosome (m), possibly unfolding as part of final disruption prior to lysis. Bar = 0.5 μm.

FIGURE 14

Electron micrograph of thin-sectioned cell 70 min after infection with phage 41c, showing final stage of lysis (Ryter-Kellenberger fixation). Cytoplasm (c) is spilling out of cell body through rupture in cytoplasmic membrane. Note double membrane (m) along upper edge of cell, believed to be fully disrupted mesosome. Some phage heads (p) are fully in plane of sectioning. Bar = 0.3 μm.

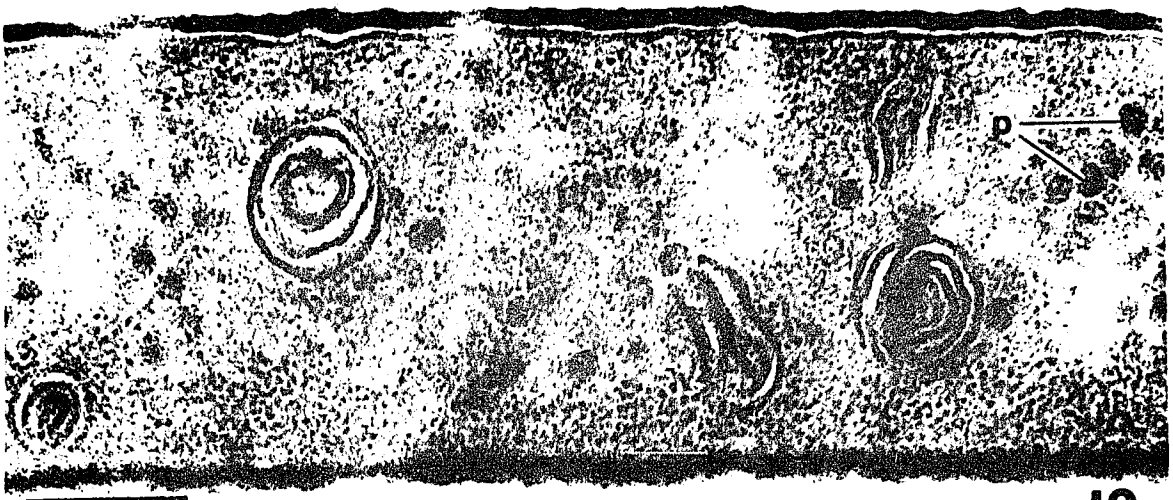

12

13

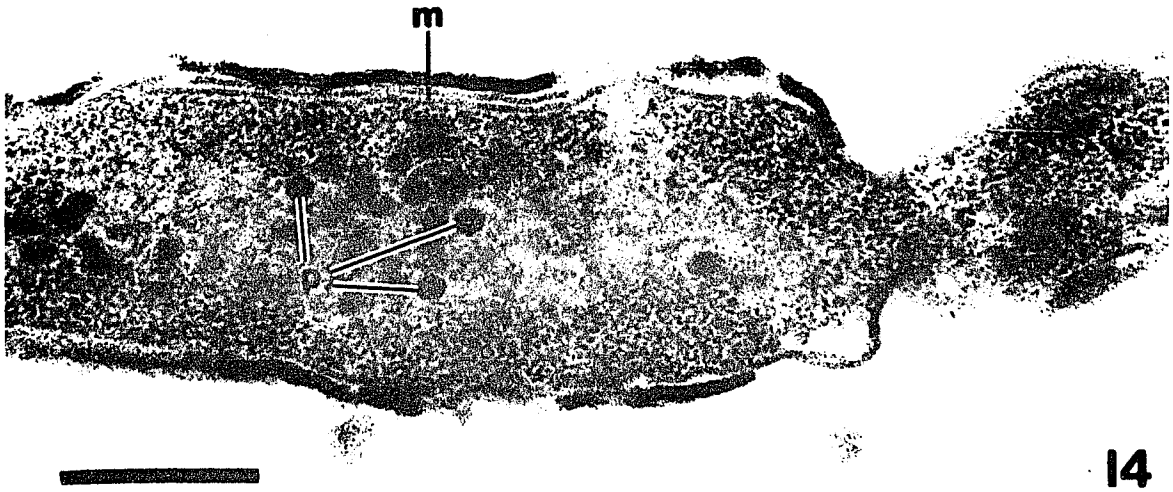

14

the number of mesosomes per longitudinal cell section increased somewhat. In contrast to cells observed between 35 and 50 min after infection, the cytoplasm of cells late in the infection sequence was quite granular. This granularity, which may have been due to the accumulation of ribosomes and/or extra capsid subunits, persisted until lysis. At the same time, the amount of nuclear material in the cytoplasm appeared to decrease.

Lysing cells were first observed approximately 70 min after infection. The peptidoglycan layer was broken down at several points around the periphery of the cell, thereby resulting in the formation of distinctive gaps in the cell wall (Figures 13 and 14). The cytoplasmic membrane apparently remained intact for some time while the peptidoglycan layer was degraded. However, it did eventually rupture at one or more of the gaps in the cell wall, thereby allowing the contents of the cytoplasm to spill out of the cell body (Figure 14). At some point during the lytic process, there was a final disruption of the mesosomes. Neither the distinctive spirals described earlier nor any other form of intact mesosome were seen in lysing cells. Instead, lysing cells appeared as though they had multiple cytoplasmic membranes. Perhaps the mesosomes unfolded completely and lined up as single membranes just inside the peripheral cytoplasmic membrane (Figure 14). It was not clear whether this final disruption of the mesosomes preceded lysis or was actually a result of it.

Fooke-Achterrath fixation. All of the ultrastructural changes described above were evident in cells preserved with the Ryter-Kellenberger procedure. Cells infected with phage 41c were also

prepared for electron microscopy by the Fooke-Achterrath technique, a fixation recommended for "close-to-life" preservation of mesosomes (20). Both uninfected cells and infected cells sampled throughout the first 35 min of the latent period were ultrastructurally identical to those fixed by the Ryter-Kellenberger method, except for the location and size of their mesosomes. The internal ultrastructural configuration of these mesosomes was the same as with the Ryter-Kellenberger method (see above), but their main bodies were peripherally located and usually did not extend into the center of the cytoplasm (Figure 9). This was in agreement with the effects reported for the Fooke-Achterrath procedure on mesosomes in Staphylococcus aureus (20). Between 35 and 40 min after infection, however, the peripherally located mesosomes in B. subtilis moved toward the center of the cytoplasm (with respect to the short axis of the cell) and began to unfold or open up. Throughout the rest of the lytic cycle, the mesosomes as well as all other cell and phage structures appeared identical to those seen with the Ryter-Kellenberger method (above). In fact, the mesosomes preserved with the Fooke-Achterrath procedure eventually took on the characteristic spiral or concentric arrangement (Figure 15), that was seen in the later portion of the lytic cycle with the Ryter-Kellenberger method (Figure 12).

Ultrastructure of Cells Infected with Phage 41c and Treated with CAP

The ultrastructure of phage 41c-infected cells which were treated with CAP at 20 min post-infection and examined by transmission electron microscopy, confirmed the results of previous

FIGURE 15

Electron micrograph of thin-sectioned cell 65 min after infection with phage 41c (Fooke-Achterrath fixation). Note presence of phage heads and distinctive, centrally located spiral or concentric mesosomes. Bar = 0.25 μm.

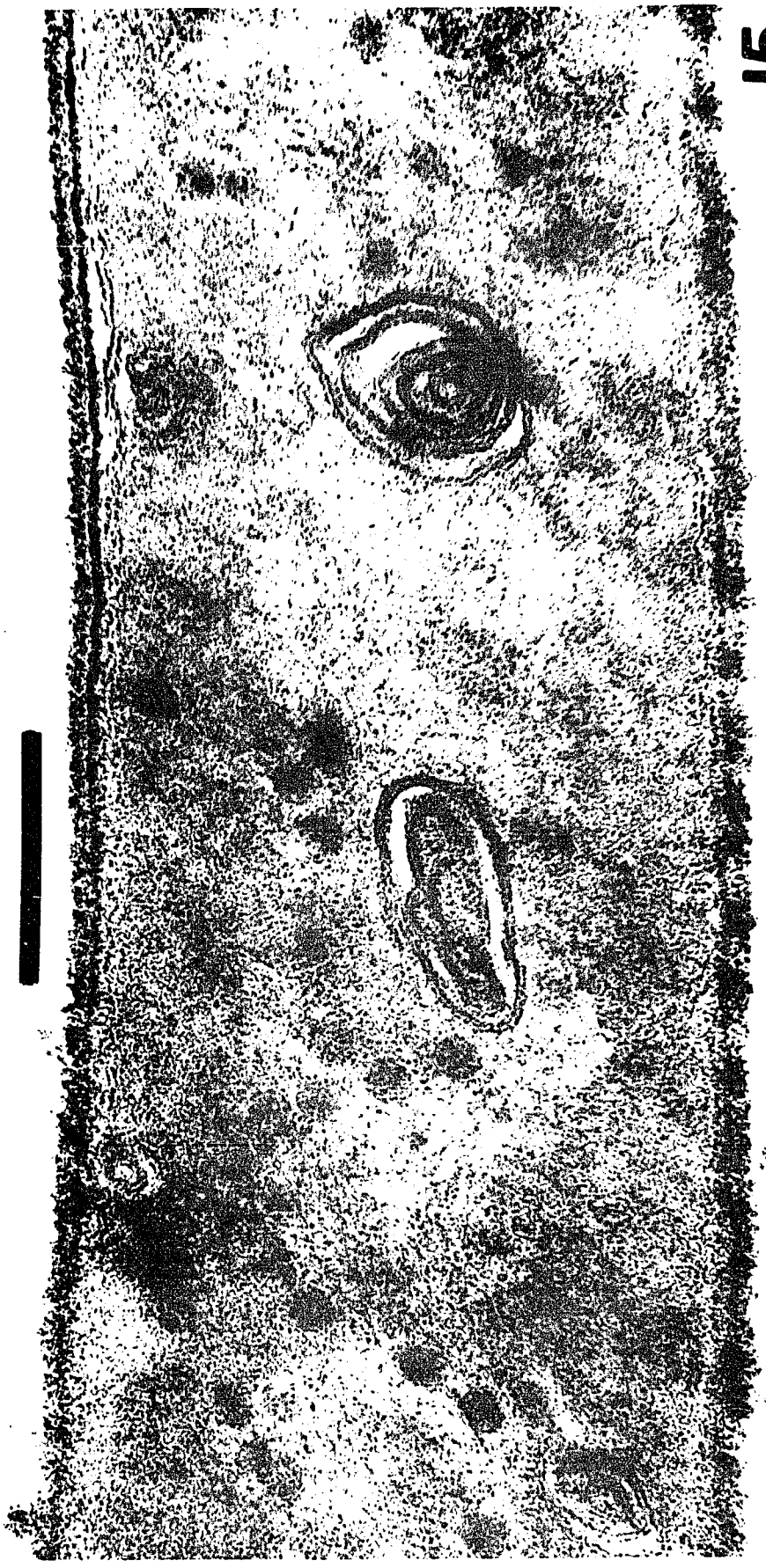

15

growth studies (see above). When CAP was added to infected cells at 20 min post-infection, mature phage were quite apparent in thin sectioned cells by 60 min post-infection. Since CAP inhibits protein synthesis, all of the necessary proteins must have been produced by the time of CAP treatment. Furthermore, the drastic alteration of mesosomes which occurred in infected cells also took place in infected cells which had been treated with the antibiotic.

Ultrastructure of Cells Infected with Phage SPP1 or SP82G

Throughout the lytic cycle, cells infected with phage SPP1 and preserved by the Ryter-Kellenberger procedure underwent morphological changes which were identical to those observed with 41c-infected cells. The apparent unfolding of mesosomes and their transition to the lamellar configuration was quite evident. As with phage 41c, SPP1 phages appeared to be preferentially associated with the mesosomal membranes for a short period of time. As phage accumulated throughout the cytoplasm, the mesosomes took on the characteristic spiral or concentric patterns (Figure 16) described above for phage 41c. All other events described for 41c-infected cells (above), including the events immediately preceding lysis were identical for phage SPP1-infected cells.

In contrast to the above, alteration or rearrangement of mesosomes was not observed during lytic infection with phage SP82G. The mesosomes within these cells often appeared to have a tightly packed tubular configuration throughout the entire period of infection (Figure 17), as did mesosomes in uninfected control cells.

FIGURE 16

Electron micrograph of thin-sectioned cell infected with phage SPP1 (Ryter-Kellenberger fixation). Cytoplasm contains many phage heads. Note distinctive spiral or concentric configuration of mesosomes. Bar = 0.3 μm.

FIGURE 17

Electron micrograph of thin-sectioned cell infected with phage SP82G (Ryter-Kellenberger fixation). Cytoplasm contains many phage heads. Note tightly packed, tubular configuration of mesosomes. Bar = 0.3 μm.

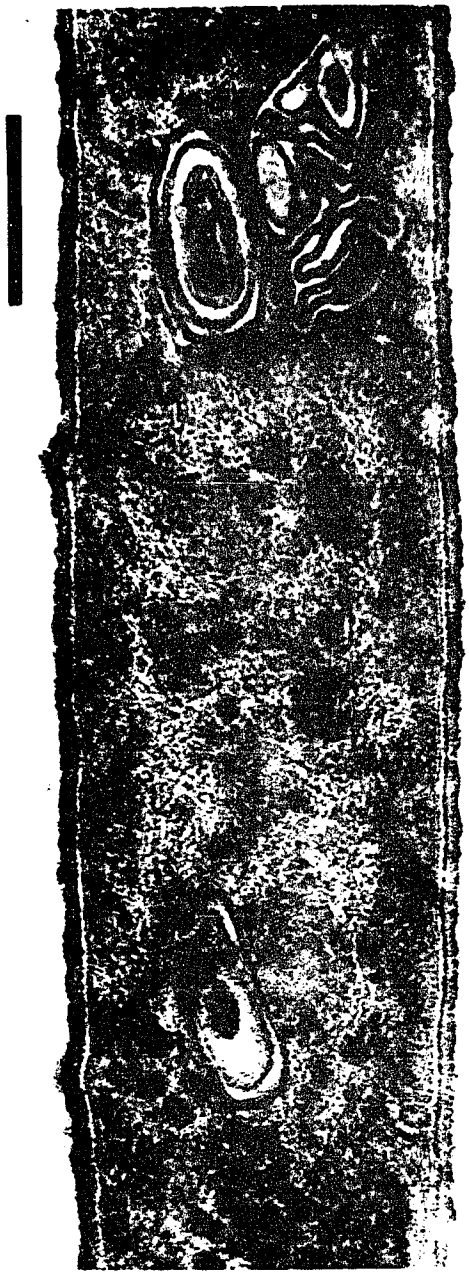

16

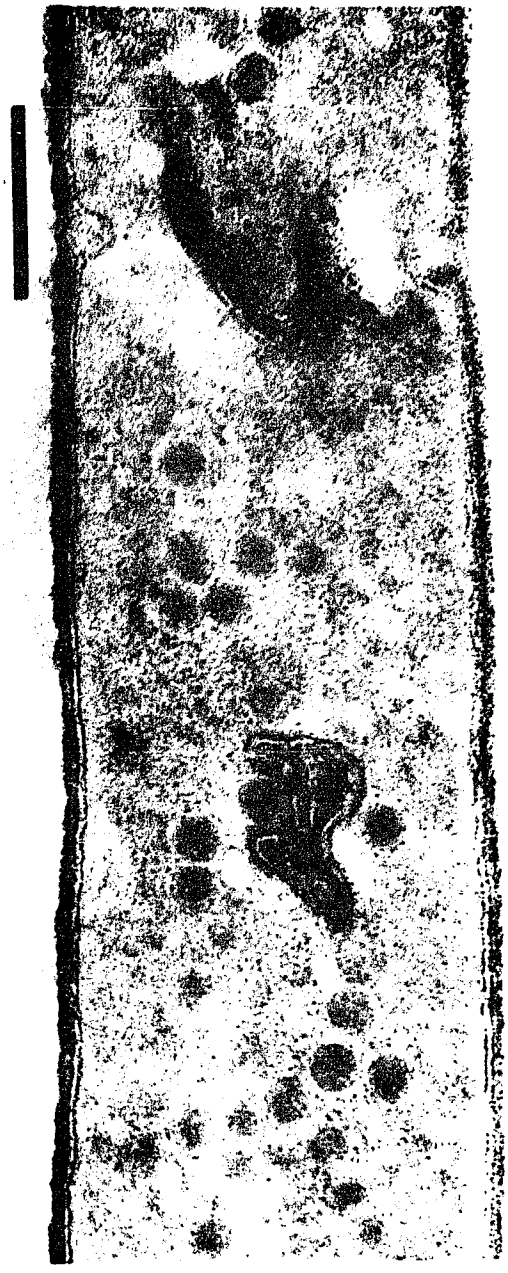

17

In contrast to the results with phages 41c and SPP1, empty heads and partially filled heads were readily apparent and clearly visible in B. subtilis cells infected with phage SP82G.

Elemental Analyses

Although the Ca^{++} detected in infected cells did not vary to any great extent from that detected in the control cells, there was a definite decrease in phosphorous and potassium (Table 9) in the infected cells as compared to the control cells.

Studies with Protoplasts

Protoplast formation and stability. The conversion of either phage 41c-infected cells or uninfected cells to protoplasts, in the presence of sucrose or sorbitol, was nearly 100% complete by 20 min after lysozyme treatment (light microscopical observations). Optical density measurements of uninfected cells indicated that the efficiency of sorbitol as a stabilizer was only about 50% that of sucrose (Figure 18). This was confirmed by direct protoplast counts. At 135 min following the addition of lysozyme and sucrose, there were 1.1×10^8 protoplasts/ml. Direct counts of protoplasts prepared in the presence of sorbitol indicated a concentration of 5.1×10^7 protoplasts/ml by this time.

The stability of protoplasts in various media was assessed by the determination of PFU/ml recovered from the protoplasts (Table 10). When 41c infected protoplasts were diluted in sucrose-supplemented TYS, all of the phage which were added to the culture were recovered. This indicated that 0.5 M sucrose was an effective stabilizer for these protoplasts. Approximately 53% of

TABLE 9

Energy-dispersive X-ray analyses

	Percent of Total Detectable Counts*					
	Na	P	S	Cl	K	Ca
Uninfected Cells	9.6	10.1	-	53.4	10.6	16.2
41c-infected Cells	8.2	4.5	0.8	64.0	4.5	17.7
SPP1-infected Cells	12.8	2.4	-	66.3	4.5	14.0

*Approximately 20,000 total counts were collected for each of the samples.

FIGURE 18

Effects of 0.5 M sucrose and sorbitol on the optical density of an uninfected protoplast suspension. Symbols: ● , sucrose added as stabilizer; ■ , sorbitol added as stabilizer. Arrows indicate 99% protoplasts.

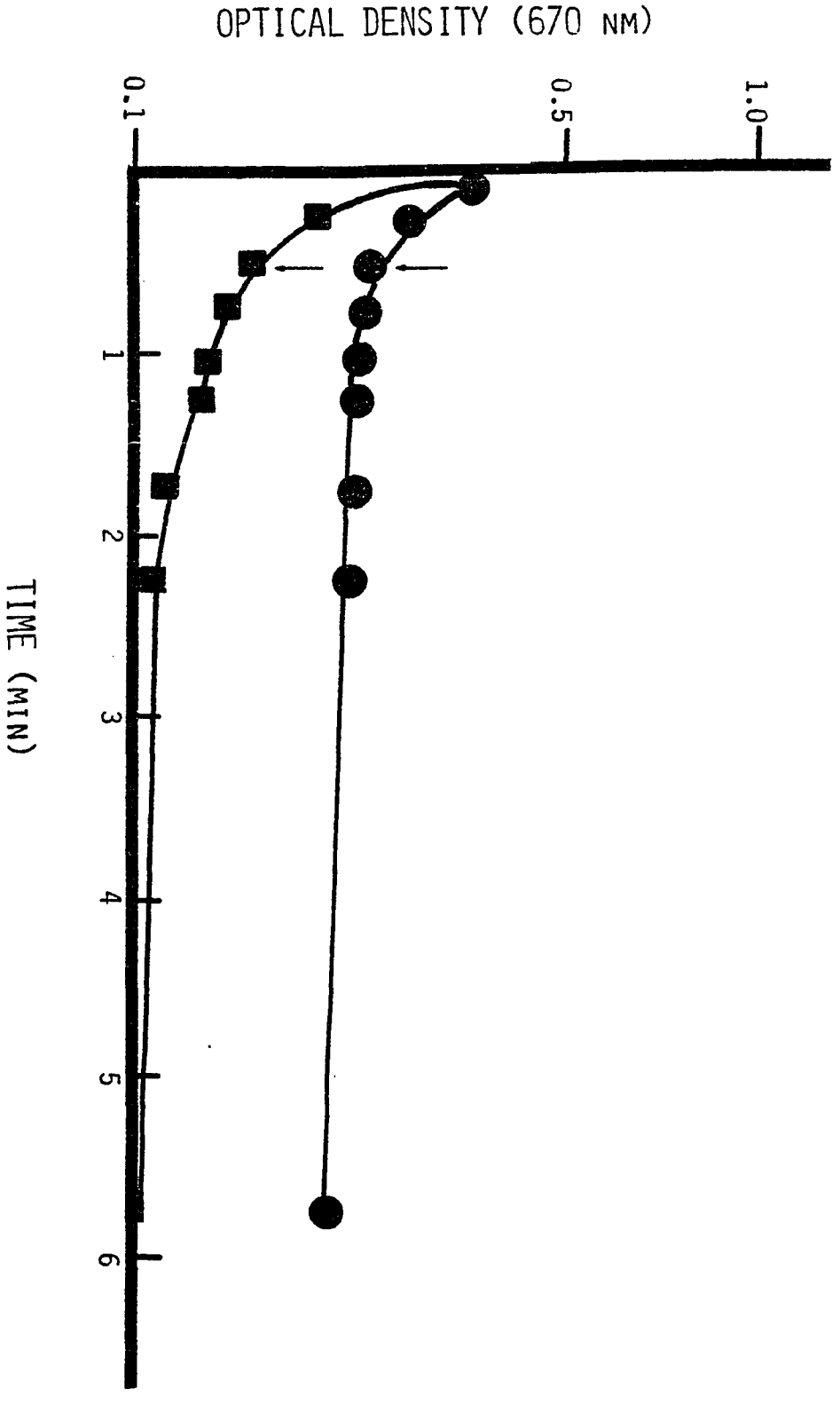
OPTICAL DENSITY (670 NM)
0.1
0.5
1.0
TIME (MIN)
1
2
3
4
5
6

TABLE 10

Phage 41c recovery from protoplasts diluted in various media*

Diluent	Basal Medium (1.5% agar)	Soft-agar Overlay (0.8% agar)	PFU/ml Recovered (Average)	Recovery of Input** (Average %)
TYS + sucrose	TYS + sucrose	TYS + sucrose	1.6×10^8	100
Saline	TYS	TYS	6.5×10^7	54
TYS	TYS	TYS	6.3×10^7	53
TYS***	TYS	TYS	3.0×10^7	25

*All media listed above were supplemented with 10 mM Ca^{++}.

**The input was determined to be 1.2×10^8 PFU/ml in intact cells. Diluent, agar plates and soft agar overlay used for input determinations contained TYS and Ca^{++}.

***Chloroform was added to the first tube of the dilution scheme to insure lysis of the protoplasts.

the phage were recovered from protoplasts which were diluted in saline or TYS broth in the absence of a stabilizer. Thus, saline or TYS contributed some osmotic stability to the protoplasts. This was confirmed by phase-contrast microscopy. Infected protoplasts, which were lysed with chloroform and subsequently diluted in TYS, resulted in a 25% recovery of the input virus. Phase microscopy revealed 100% lysis of the protoplasts. Since phage 41c is chloroform resistant, these results indicated 75% efficiency for phage adsorption and DNA penetration by 15 min post-infection in whole cells.

Replication of phage 41c in protoplasts. Although intact cells of B. subtilis infected with phage 41c produced a burst of approximately 10^3 phage per host cell, lysozyme treated cells (protoplasts) produced a much smaller burst size. Cells which were treated with lysozyme and sucrose at 15 min following initiation of infection produced a burst which was only 1% that of the intact cells. Protoplasts stabilized with sucrose and subsequently lysed with chloroform immediately prior to the plaque assay never produced a burst greater than 2% that of intact cells. It is not known whether the entire population of protoplasts allowed phage replication at a 2% efficiency or if 2% of the infected protoplasts produced a normal burst of phage. In the latter case, it is possible that 1-2% of the infected cells escaped lysozyme treatment. In any event, the lytic cycle which took place in these sucrose-stabilized protoplasts exceeded 7 h (Figure 19). In contrast, the 41c lytic cycle in protoplasts was completed within 2 h when sorbitol

FIGURE 19

Growth curve of phage 41c in sucrose-stabilized protoplasts. Symbols: ● , protoplasts stabilized by the addition of 0.5 M sucrose in diluent, basal media, and soft-agar overlay; ■ , protoplasts diluted and assayed in TYS media without sucrose.

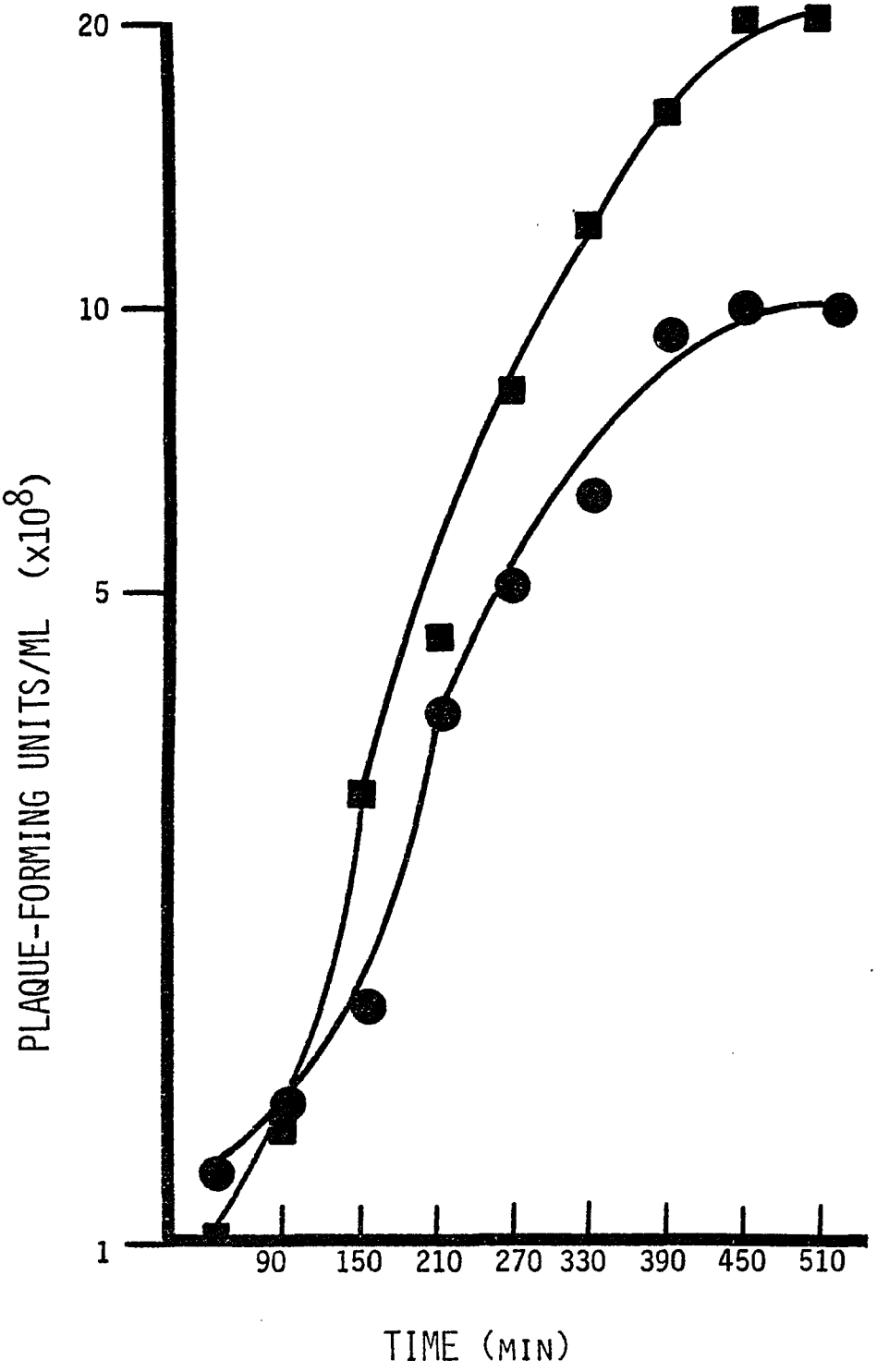
20
10
5
1
PLAQUE-FORMING UNITS/ML (x10^8)
90
150
210
270
330
390
450
510
TIME (MIN)

was substituted for sucrose (Figure 20). The burst size was larger than that which occurred with sucrose-stabilized protoplasts, yet it was only 25-30% that of the burst size in intact cells. This may have been partially due to the spontaneous lysis of protoplasts prior to phage replication. Similar to the results with sucrose, the number of phage recovered from infected protoplasts which were stabilized with sorbitol and lysed with chloroform prior to plating did not differ from that of protoplasts which were handled gently. Apparently protoplasts which contained mature phage were not protected from lysis by either sucrose or sobitol.

Ultrastructure of uninfected protoplasts. Protoplasts which were prefixed with glutaraldehyde appeared similar in ultrastructure to those which have been described previously (46,48). They were generally spherical in shape, although ovoid forms were sometimes observed when wall degradation was incomplete. Spherical forms varied in diameter from 1.5 to 2 μm, but averaged 1.7 μm. The cytoplasmic membrane was usually quite evident (Figure 21), as was the extrusion of mesosomes into the extracellular environment. The extruded mesosomes always appeared vesicular in configuration. Membranous material was rarely observed in protoplasts which were totally devoid of wall material. Furthermore, the nucleoplasm and cytoplasmic portions of the protoplasts were usually well defined. The nucleoplasm appeared as an electron-transparent region within the protoplasts and usually occupied about one-half the area contained within the cytoplasmic membrane. The cytoplasm

FIGURE 20

Growth curve of phage 41c in sorbitol-stabilized protoplasts. Symbols: ● , protoplasts stabilized by the addition of 0.5 M sorbitol in diluent, basal media, and soft agar overlay; ■ , protoplasts lysed with chloroform prior to assay in TYS media without sorbitol.

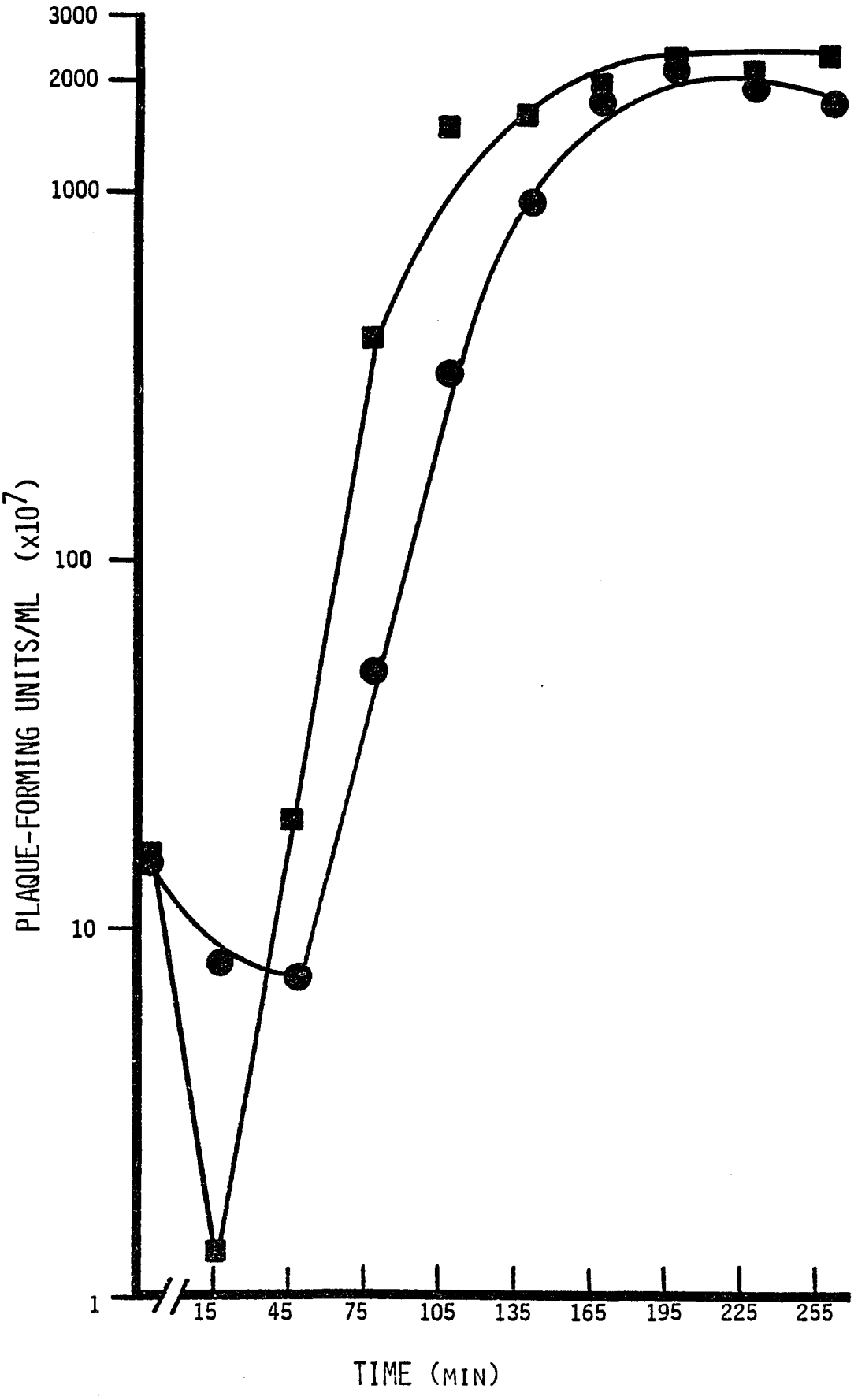
3000
2000
1000
100
10
1
PLAQUE-FORMING UNITS/ML (x10^7)
15
45
75
105
135
165
195
225
255
TIME (MIN)

FIGURE 21

Electron micrograph of thin-sectioned, uninfected protoplasts. Note the extrusion of mesosomes from the protoplasts. Prefixed in 1.25% glutaraldehyde in the presence of 0.5 M sucrose. Bar = 1 μm.

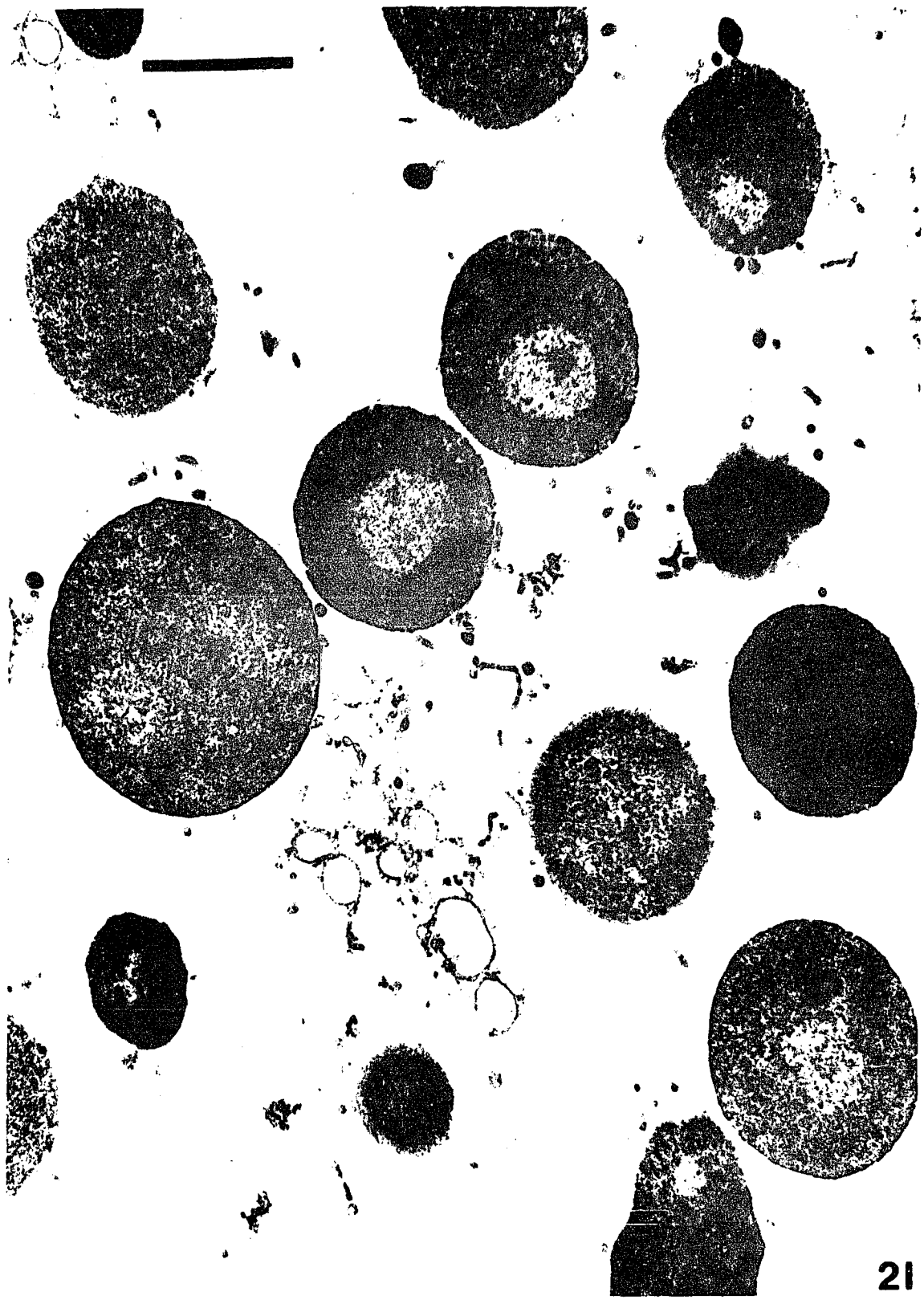

21

of uninfected protoplasts was electron-dense and appeared relatively smooth in consistency.

Ultrastructure of protoplasts infected with phage 41c. The ultrastructure of protoplasts infected with phage 41c was identical to that of uninfected protoplasts until phage appeared within them. Although the samples were treated with both CAP and lysozyme, intact phage were first observed in samples taken at 40 min post-infection (Figure 22). The phage appeared as spherical, electron-dense particles just as they did in whole cells infected with phage 41c. In contrast to those in whole cells, however, the phage particles in protoplasts never appeared to be membrane-associated. Instead, the vesicular mesosomal membranes were extruded from the protoplasts while the phage remained inside. In fact, the phage were usually located on or close to the periphery of the nucleoplasm. As was the case in infected whole cells (above), the cytoplasm of the protoplasts became rather granular in consistency as phage accumulated. Perhaps this was due to an excess accumulation of viral protein subunits and/or ribosomes. The latter were usually visible within mesosomes.

An interesting observation was made when samples were taken from a 41c-infected culture during the latter part of the lytic cycle in the absence of antisera to the phage. Since most of the protoplasts lysed as a result of phage infection, there was an excess of cellular debris (particularly membranous material and phage progeny). The phage within the sample demonstrated a strong affinity for the membranous debris (Figure 23). Since

FIGURE 22

Electron micrographs of thin-sectioned protoplasts treated with chloramphenicol and lysozyme 40 min after infection with phage 41c. Phage are located within the periphery of the nucleoplasm, while mesosomes are extruded outwards. Prefixed with 1.25% glutaraldehyde in the presence of 0.5 M sucrose. Bars = 0.5 μm.

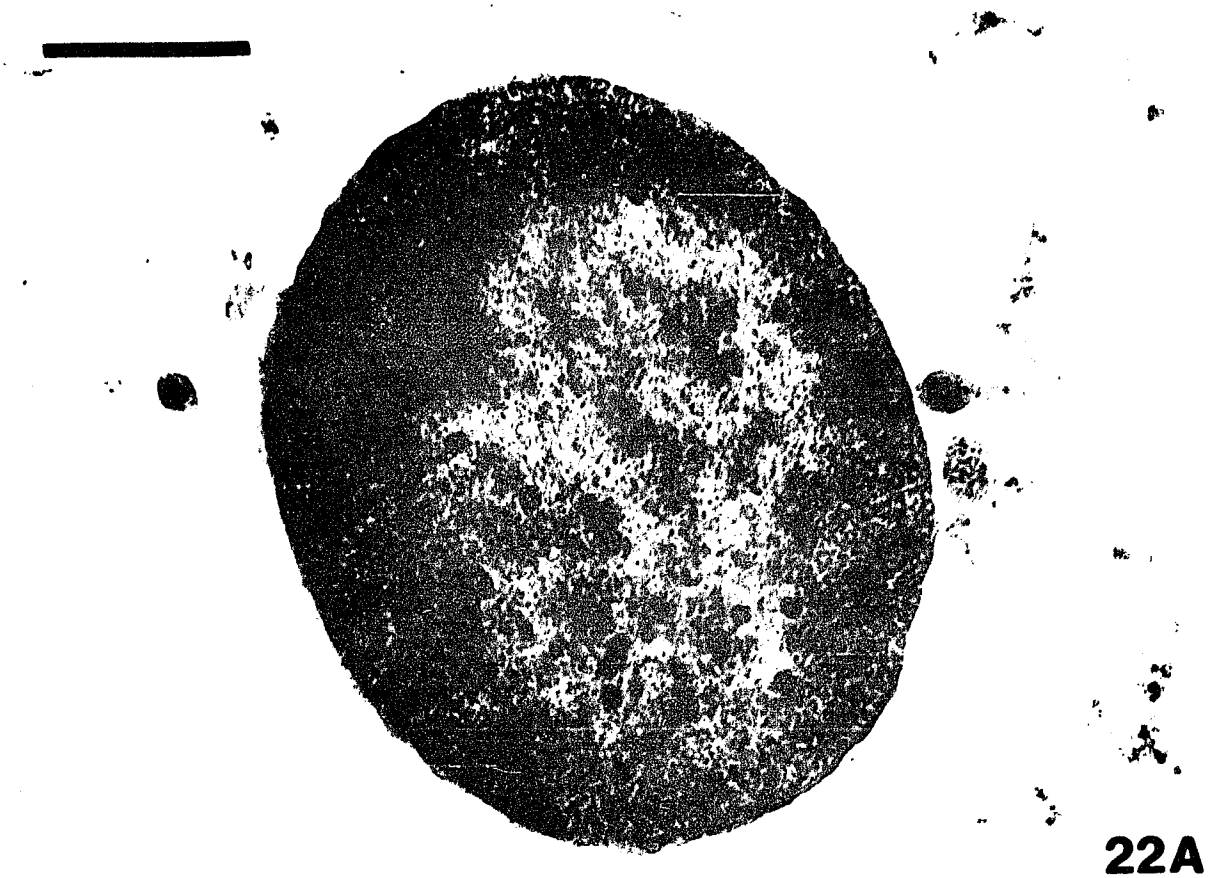

22A

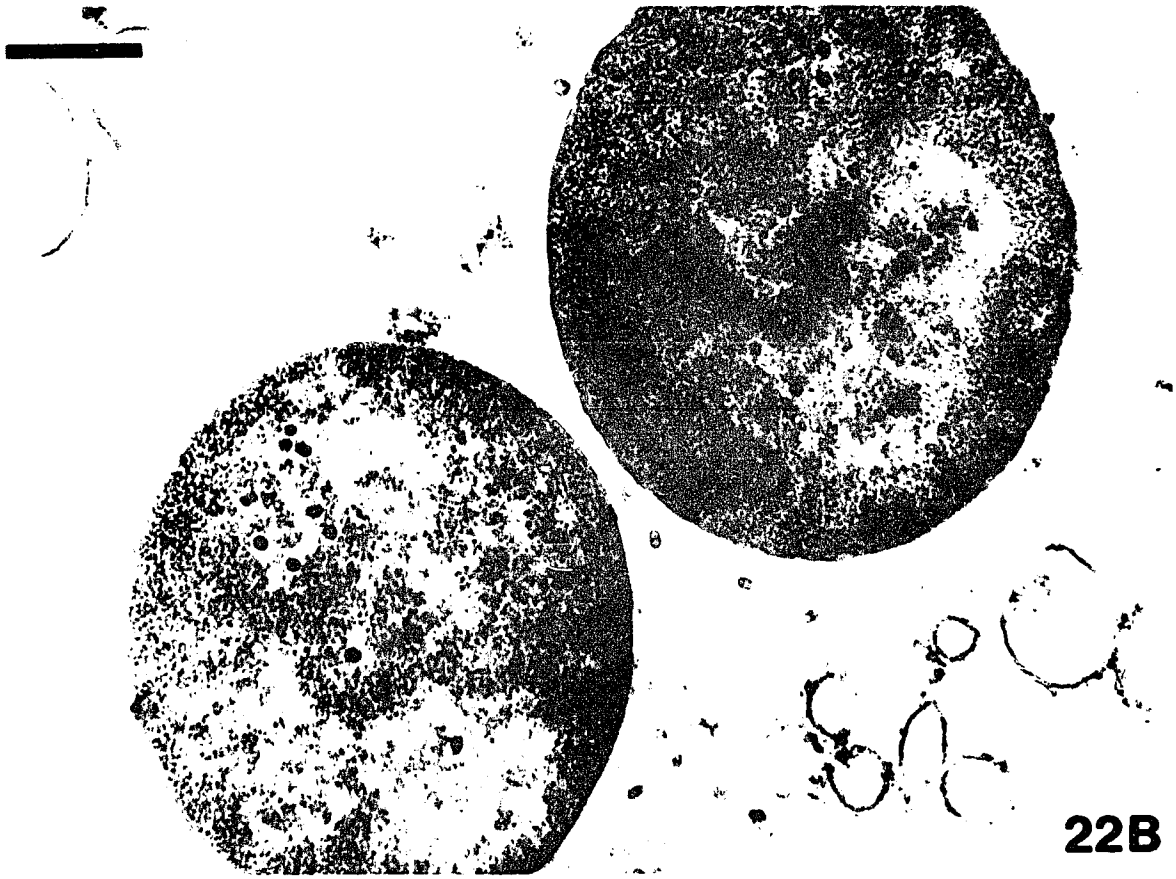

22B

FIGURE 23

Electron micrographs of phage 41c attachment to membranous debris. Prefixed with 1.25% glutaraldehyde in the presence of 0.5 M sucrose. Bars = 0.5 μm.

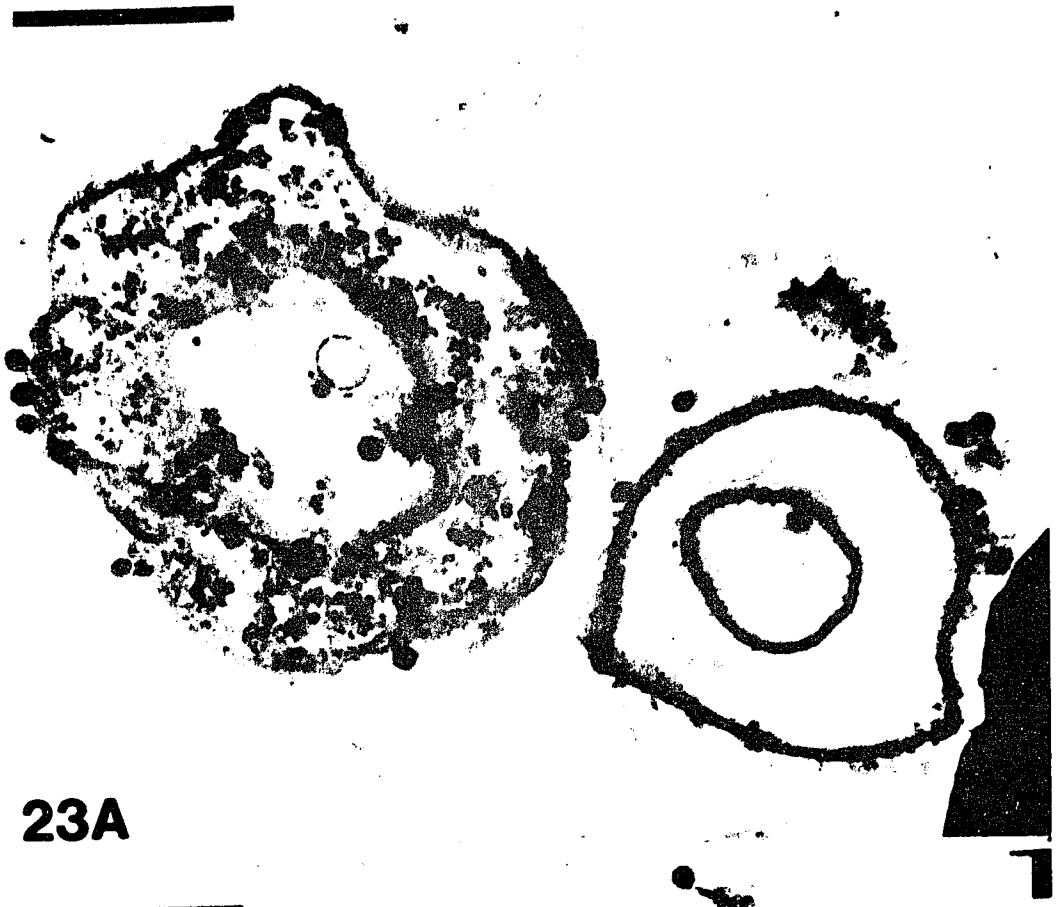

23A

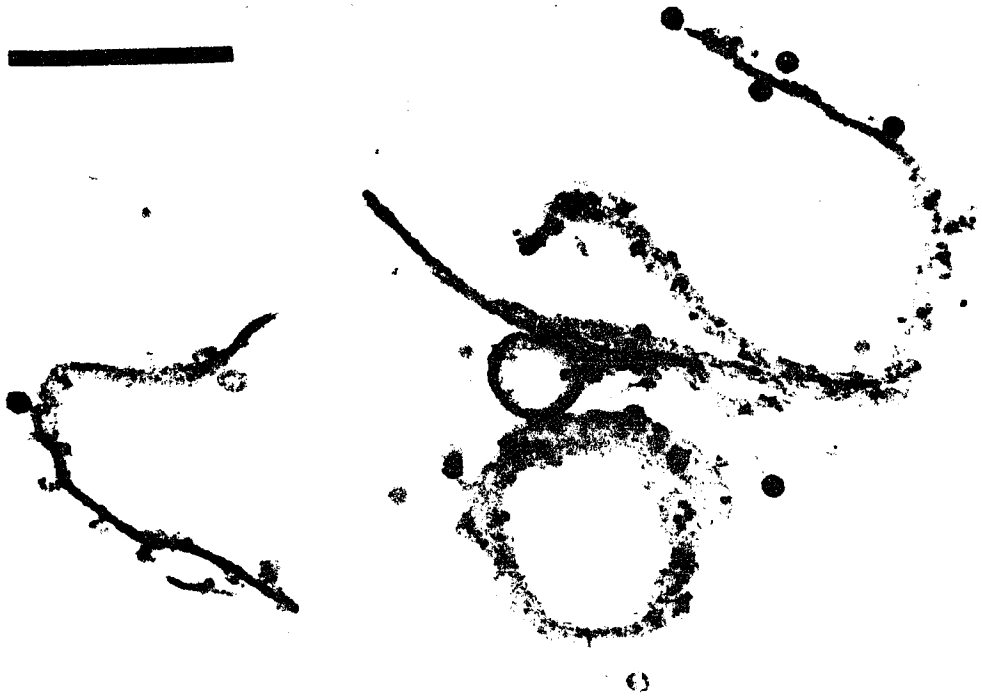

23B

this phenomenon was not observed in samples previously treated with antisera to phage 41c, these data suggest that receptor sites for phage 41c are on host membranes.

V. DISCUSSION

Characterization Studies

Phage 41c, originally isolated from soil (93), is a highly virulent phage for Bacillus subtilis 168. At the onset of this characterization study, it was apparent that there were significant similarities between phages 41c and SPP1, another phage specific for B. subtilis 168 (26). The phages were almost identical in head and tail dimensions, tail flexibility, head morphology, and mole % G+C (64,93). They also shared a similar density pattern for the light and heavy strands of their DNA. The calculated densities of the light and heavy bands of phage 41c DNA were 1.714 g cm^{-3} and 1.724 g cm^{-3}, respectively (92). In comparison, the light and heavy bands of phage SPP1 DNA were 1.713 g cm^{-3} and 1.725 g cm^{-3}, respectively (64). Intact DNA extracted from either phage had a density value of 1.703 g cm^{-3} (64,92). In addition, the molecular weights of their respective DNA molecules were quite similar: 3.0×10^7 daltons for phage 41c (92) and 2.5×10^7 daltons for phage SPP1 (64).

In view of the similarities between phages 41c and SPP1, a more detailed comparative study of these phages was deemed necessary. The results of this study indicate that phages 41c and SPP1 are remarkably similar. Neither phage contained unusual bases in their DNAs, although the presence of thymine was not

apparent in chromatographic analyses of phage 41c DNA. Since ^{3}H-thymidine was incorporated into phage 41c DNA as it was in SPP1 DNA, and nuclear magnetic resonance (NMR) spectroscopy of phage 41c DNA indicated that thymidine was present, the results of chromatographic analyses remain unexplained. NMR spectroscopy of phage DNA did not reveal the presence of uridine (68) and it is therefore unlikely that phage 41c contained both of these pyrimidines. Perhaps the methyl group which distinguishes thymine from uracil was cleaved from the molecule during the formic acid hydrolysis used in this study. There are no reports of this in the literature, however.

Phages 41c and SPP1 exhibited a comparable sensitivity to blockage of infection by DNase or streptomycin. Although the former was shown to interfere with phage 41c-DNA penetration during infection (93), the latter probably competes with the phage for the Ca^{++} (R.M. Zsigray, personal communication). Other similarities between the phages included a limited host range and poor plaquing efficiency in the absence of Ca^{++}. Since Landry and Zsigray (41) showed that 41c has a specific Ca^{++} requirement for adsorption, penetration, and intracellular development, it is likely that phage SPP1 also has a similar requirement.

Based on the K values (velocity constants) for antisera produced against phage 41c, the phages were related serologically as well. The difference in K values was less than that which was found between the K values of closely related T-even phages (200, 50, and 90 for T2, T4, and T7 respectively; ref. 1). The antigenic similarity between phages 41c and SPP1 was, therefore,

unquestionable.

Polyacrylamide gel electrophoresis revealed a similar pattern of protein subunit molecular weight distribution for disrupted concentrates of phages 41c and SPP1. A minimum of 15 bands was clearly resolved for both phages. The molecular weight determinations for phage SPP1 were in partial agreement with those previously reported for SPP1 by Esche et al. (17) who identified 10 structural proteins for SPP1 among a total of 23 viral-directed proteins (Appendix). Although at least 15 distinct subunits were detected in our experiments, only 4 of these could be matched with the structural proteins described by Esche et al. (17). These were presumably products of gene M18 (a head protein) and genes M10, M13, and M19 (all tail proteins). The main difference between 41c and SPP1 in our gel patterns was that the former possessed a protein with a molecular weight of about 54,000 daltons that was absent in SPP1, while the latter possessed a protein with a molecular weight of about 41,500 daltons that was absent in 41c. Other small differences in protein concentration were also observed, but the significance of these differences is unclear. Presumably, gene products M14, M16, and M17 (17) were too low in molecular weight to be resolved by our gel system. In addition, M11, M12, and M15 proteins were not detected by our gel system. They may have been present in a concentration too low to be observed, but this seems unlikely because M15 was reported to be a major protein subunit for SPP1 (17). Increasing the concentration of sample in our gels resulted in excessive trailing and indiscrete bands. Nevertheless, proteins which Esche et al. (17) proposed to be non-structural

were consistently apparent in our gels. According to their data, products which corresponded to genes E2, E3, M20, M22, L30, L33, and $C_{(y)}$ were present in our phage preparations. We also detected three proteins which were not reported previously. Since the virus concentrates were washed three times with sterile saline by ultracentrifugation and then filter sterilized prior to disruption, we believe these represent structural proteins. Perhaps the discrepancy can be attributed to the methods used for phage disruption. In this study, heat was used to disrupt the structural proteins, as opposed to chemical treatment with DMSO followed by ultracentrifugation to separate heads and tails (17). It is possible that proteins involved in head-tail attachment and, perhaps, internal proteins were lost during the centrifugation step. The two methods could not be compared directly because attempts to separate heads and tails by ultracentrifugation following chemical denaturation were unsuccessful in this laboratory. On the other hand, it is possible that the resolution of four bands in this study (corresponding to molecular weights of 43,000, 41,500, 40,000, and 38,000 daltons) were reported as two bands (corresponding to molecular weights of 42,000 and 39,000 daltons) by Esche *et al.* (17). The consistent appearance in our gels of a previously unreported protein possessing a molecular weight of about 66,000 daltons remains to be explained.

Phages 41c and SPP1 produced plaques with strikingly different morphologies. However, this was not sufficient to characterize them as separate entities, since mutant strains of phage SPP1 have been reported to vary in their plaque morphologies (76).

Nevertheless, these differences proved valuable in determining the outcome of simultaneous infection of B. subtilis with phages 41c and SPP1. Others (56) have studied the progeny released from B. subtilis infected simultaneously with unrelated phage and have found that these phage can be ranked in a hierarchial order in terms of their ability to dominate infections. However, exclusion of either phage 41c or SPP1 by the other was not observed, thereby suggesting a close relatedness between them. Due to the numerous similarities between phages 41c and SPP1, it is suggested that phage 41c be included in Group 5 of the B. subtilis bacteriophages as proposed by Hemphill and Whiteley (26).

Physiological Studies

Enumeration of phage 41c during lytic infection of B. subtilis 168 indicated a latent period of about 50 min and a burst size of approximately 10^3 phage per host cell. Although this latent period was similar to those reported for other B. subtilis phages, the burst size was not. Compared to those of most other phages, the burst size of phage 41c was strikingly larger (23, 38,54,61,90). The largest burst size reported previously for a B. subtilis phage was that of Ø29, which had a burst of 570 phages per host cell (70). Like Ø29, phage 41c may prove to be a valuable tool for genetic studies. Previous work with phage SPP1 has already demonstrated the importance of that phage in studies on host competence, phage recombination, and transfection (63,76,77).

Phage 41c is not only a virulent phage in terms of its burst size, but it is also efficient in its synthesis of protein. The addition of chloramphenicol to phage 41c-infected cells after 30 min of infection did not prevent lysis of 75% of the cells. Thus, structural protein synthesis was probably complete by this time. However, the degree of lysis was dependent on the time that the antibiotic was added to the infected cultures. This was probably a result of staggered phage adsorption, since phage which would have adsorbed 5 min later than others would still need time to synthesize proteins. In addition, it is possible that late functional proteins such as lysozyme were not synthesized in suitable amounts to lyse the cells. According to Esche et al. (17), the synthesis of late functional proteins does not begin until about 25 min after infection by phage SPP1. Their data are in agreement with that for phage 41c; i.e., maximal synthesis of phage structural proteins occurred by 20 min post-infection. In addition, intact phage were not found in thin sections of phage 41c-infected cells by 20 min after infection, but were quite evident by 60 min post-infection (even when protein synthesis was stopped at 20 min). These observations most likely indicate that phage assembly was the most significant event that occurred between 20 and 60 min post-infection in these experiments. In vivo, proteins were probably being synthesized continuously during this period. This would ultimately result in more phage per host cell, more lysozyme produced, and therefore, more lysis of cells.

Phage SPP1 was shown to develop in the presence of active

host functions (16). In that study, the inhibition of host DNA synthesis by hydroxyphenyl-azo-uracil (HPUra) also inhibited phage SPP1 DNA replication. Furthermore, the host enzyme, glycerolphosphate dehydrogenase could be induced at all times after infection (16). Results reported in this dissertation indicated that a 41c-infected culture of B. subtilis increased in optical density until lysis began. In addition, the rate of ^{3}H-thymidine uptake in 41c-infected cells was about the same as that of SPP1-infected cells. Since both host and phage macromolecular syntheses were probably occurring, there was undoubtedly competition between phage and host for cell machinery. Thus, infected cells did not take up the label at a higher rate. Toward the latter portion of the lytic cycle, uninfected control cells appeared to take up the nucleotide at a higher rate. However, this was probably not actually occurring because infected cells began lysing by that time.

The continuity of host DNA synthesis during phage infection in B. subtilis is not unusual, although it does differ from the events which occur during phage infection in E. coli. In T-even phage infections, there is a rapid shut-down of host syntheses, followed by degradation of host DNA (26). Infection of B. subtilis by large phages such as SP82G, SP01, Ø25, and SP8 results in the gradual decrease of host macromolecular synthesis, without the breakdown of host DNA (26,65,91). Nevertheless, infection of either B. subtilis or E. coli by small phages (Ø29 and T7, respectively) has little effect on host functions (26). In view of the size of phage 41c, it is not surprising that it did not affect host replication.

Ultrastructural Studies

These studies have served primarily to illustrate the ultrastructural changes which occurred in B. subtilis during lytic infection with the double-stranded DNA phage 41c. The effects of phage SPP1, as well as those of a dissimilar phage, SP82G, on the appearance of mesosomes in host cells were also examined.

In 41c and SPP1-infected cells, a rather distinct change in the ultrastructure of the host cell itself was seen prior to the appearance of phage structures. The mesosomes in these infected cells not only opened up and spread throughout the cytoplasm, but also underwent a change in configuration from vesicular to lamellar. They contracted to some extent and took on a distinctive spiral or concentric form later in the lytic cycle. These changes appeared to be a direct result of the phage infection itself, rather than an effect of the procedures used to prepare the cells for electron microscopy. The alterations were observed in cells (infected in the presence of Ca^{++} or Ca^{++} and Mg^{++}) preserved with the Ryter-Kellenberger procedure, or with the Fooke-Achterrath technique that has been recommended for "close-to-life" preservation of bacterial mesosomes (20). The central location of mesosomes in cells sampled from the later portion of the lytic cycle and prepared by the Fooke-Achterrath method suggested that the effects of 41c actually negated the usual tendency of this procedure. Although mesosomes appeared as peripheral structures in uninfected cells, the mesosomes became centrally located during the latter portion of the lytic cycle.

In contrast, the host cell mesosomes of B. subtilis were not rearranged or altered during infection with phage SP82G. The mesosomes maintained a tubular internal configuration throughout the infection cycle, as did those of the uninfected cells. This internal configuration was somewhat different from that seen with other uninfected cultures, probably because all cells for the SP82G experiments were grown in the presence of added Mg^{++}. It should be noted in this regard that the in vivo configuration of mesosomes is currently a matter of controversy (10,20,22,27,51, 73). Therefore, the results of this study did not necessarily illustrate the true internal substructure of B. subtilis mesosomes, either before or after infection. Nevertheless, it was clear from our results that a marked change in mesosomal configuration took place as a result of phage 41c or SPP1 infection and that this change was not seen during infection with phage SP82G.

The phage-induced rearrangement of host cell mesosomes described in this study is a novel observation. It has not been reported to occur in any of the extensively studied Gram-negative host-phage systems. Investigations dealing with the ultrastructure of lytic infections in Bacillus (2,3,43,81) have not reported alterations of mesosomes either. This may indicate that the phenomenon is limited to a few phages such as 41c or SPP1. However, the relative paucity of detailed ultrastructural studies on Gram-positive host-phage interactions precludes a definite statement to this effect at present.

The way in which mesosomes of B. subtilis were altered during the lytic cycle is not known, although it is unlikely that they

were altered as a consequence of protein synthesis. The mesosomes remained vesicular in structure when sampled at 20 min post-infection, following the addition of chloramphenicol. It is also unlikely that these changes resulted from phage DNA attachment to membrane surfaces. Although studies with phage Ø29 (31) and other viruses (26) have indicated that the DNAs of all B. subtilis phages probably bind to the membrane before they undergo replication, the alteration in mesosomes was not observed in phage SP82G-infected cells. Elemental analyses indicated that there was a definite decrease in the phosphorous and potassium contents of infected cells in comparison to those of uninfected cells. Since a decrease in the intracellular potassium concentration has been correlated with a decrease in the osmotic tolerance of a cell (13) it is likely that the cell membranes were no longer maintaining "normal" ionic conditions within the cell. This may have been due either directly or indirectly to phage infection. Association of phage replication with the host membranes could have resulted in membrane deterioration simply due to physical stress. On the other hand, competition for the ribosomes by both cell and phage directed mRNA, might have resulted in a decreased synthesis of membrane structural proteins. Since proteins account for more than one-half of the dry weight of the cell membrane (79), it would not be surprising to find that the membranes became more permeable to some solutes. The resulting osmotic or chemical changes in the cytoplasm could have led to the rearrangement of the mesosomes seen during infection with 41c or SPP1. Indications that plasmolysis occurred late in the lytic cycle, further support

this possibility. Since calcium and phosphorus concentrations have been shown to affect the structure of mesosomes (10,73), it is possible that the loss of potassium and phosphorous from infected cells was the specific cause of mesosome rearrangements.

At the onset of this study, it appeared feasible that phage assembly was membrane-associated, especially since: (i) phage appeared to be preferentially mesosome-associated early in the lytic cycle and (ii) phage replication was markedly decreased in B. subtilis protoplasts when compared to replication in intact cells. However, the extrusion of mesosomes from protoplasts (prepared from infected cells) never revealed a time at which the phage were attached to the extruded mesosomal membranes. Yet, they did show affinity for membrane fragments. Since it is possible that phage-membrane association was a very short-lived arrangement, more frequent sampling might have detected such an association. Replication in sorbitol-stabilized protoplasts was more efficient than it was in sucrose-stabilized protoplasts, probably due to a general decrease in macromolecular syntheses in the latter. Perhaps the additional energy required by the protoplasts for maintaining its integrity in the absence of the cell wall accounted for the decreased phage replication in all protoplasts as compared to intact cells.

The most extensive ultrastructural and physiological studies on the intracellular development of B. subtilis phages to date are those describing phage Ø25 by Liljemark and Anderson (43) and phage Ø29 by Nelson et al. (52). Several differences in the

comparative ultrastructural effects of lytic infection by phages 41c or SPP1 vs. those described for ϕ25 and ϕ29 were detected in addition to the rearrangement of mesosomes (seen with 41c and SPP1, but not with ϕ25 and ϕ29). Neither empty particles nor partially filled particles were ever clearly observed during the development of phages 41c or SPP1, although they were frequently found in electron micrographs of cells infected with phages SP82G, ϕ25 (43) and ϕ29 (52). However, Nelson et al. (52) did not feel that the empty heads were true intermediates in the morphogenesis of phage ϕ29. In contrast, Liljemark and Anderson (43) suggested that the empty heads and partially filled heads represented true intermediates of phage ϕ25 maturation. These ultrastructural differences probably indicate that both phages 41c and SPP1 have a mechanism for intracellular development that is somewhat different from that used by most other B. subtilis phages. This conclusion is supported by physiological data, as well. Unlike phages ϕ25 (43) and SP82G (65), phages 41c, SPP1, and ϕ29 (52) did not readily interfere with host macromolecular synthesis.

In addition to information on phage replication, this study has provided documentation of the ultrastructural changes that occur within the host cell itself during the process of lysis. Our observations on the initial lytic events were similar to those of other investigators for both Gram-negative and Gram-positive cells. Wyckoff (88) reported that the cell wall of E. coli B disintegrated early during lysis, while the cytoplasmic membrane remained intact. Other studies of infected Gram-

positive cells have led to similar conclusions (8,43). The cell wall was broken down at several points around the periphery of the cell. This was also evident in B. subtilis cells which lysed as a result of infection by ∅25 (43). In addition, thin sections of several lysing cells (infected with phage 41c) indicated the complete disruption of mesosomes. This latter phenomenon has not been described in other investigations on lysing cells. Abrupt changes in osmotic pressure as the cytoplasmic membrane ruptured may have caused the final perturbation of mesosomes observed in this study. It was also possible to find several examples of cells in the process of lysing even though the chances of preserving and obtaining informative sections through such cells are quite poor. These electron micrographs confirmed that the cytoplasmic membrane eventually did burst at one or more of the gaps formed previously in the cell wall.

The examination of lysozyme-treated B. subtilis cells clearly demonstrated the extrusion of mesosomes away from the cell during protoplast formation (19). These mesosomes contained small electron-dense, spherical particles believed to be ribosomes (46). In addition, the cytoplasmic membrane was clearly intact and the nucleoplasm was quite evident. Apparently the protoplasts were chemically preserved without much cellular distortion. Although the presence of phage in infected protoplasts was quite obvious, the phage were never in close association with the mesosomes. Instead, they usually appeared at the periphery of the nucleoplasm. The frequency at which phage-containing protoplasts were observed indicated that phage did replicate in

protoplasts when allowed sufficient time for adsorption and penetration in intact cells. The decreased burst size was consistent with that reported by Brenner and Stent (9) for replication of phage C in sucrose-stabilized protoplasts. They reported a burst size of 1% of that of intact cells, found that at least half of the infected protoplasts produced phage, and found that the individual bursts were small. Results of similar experiments described by Salton and McQuillen (69) indicated the growth of phage C in B. megaterium protoplasts gave a maximum phage yield which was one-seventh that of intact organisms. They considered this to be quite high in view of the inability of protoplasts to divide in broth medium. Nevertheless, rates and phage yields varied from one experiment to another, probably due to the physiological state of the protoplast cultures (69). Apparently, protoplasts retained sufficient structural organization to support the growth of bacteriophages. However, it is difficult to assess the role of mesosomes during phage 41c assembly since, by definition, the formation of protoplasts necessarily results in the extrusion of mesosomes.

An interesting observation was made during the preparation of protoplasts from B. subtilis cells which had been infected for 60 min. The extracellular phage demonstrated a strong affinity for the membranous debris (in the absence of antisera), suggesting the presence of receptor sites on the host membranes. This was not overly surprising, since Jacobson and Landman (32) reported the ability of a variety of B. subtilis phages (including phages 41c and SPP1) to plaque on both walled and wall-less forms of

B. subtilis. These authors suggested that the attachment sites in the wall and in the membrane are essentially the same for these phages. In addition, they reported that phage 41c adsorption to B. subtilis protoplasts resulted in productive lysis, although no data pertaining to the burst size was published (32).

Based on data pertaining to mesosome alterations and other ultrastructural observations, DNase sensitivity (93), and multi-requirements for Ca^{++} (41), it seemed reasonable to conclude that phage 41c has an unusual, yet complex method of DNA penetration, and intracellular development.

SUMMARY

Results of this investigation indicated that phage 41c was remarkably similar to phage SPP1, another phage specific for Bacillus subtilis. The phage were identical in morphology and dimensions, buoyant densities of their separated DNA strands, incorporation of ^{3}H-thymidine into their DNA, sensitivity of infection to deoxyribonuclease or streptomycin, host range, and plaquing efficiency. Slight differences were detected in the molecular weights of their structural protein subunits and plaque morphologies. Mixed infection of B. subtilis by phages 41c and SPP1 did not result in the exclusion of either phage, thereby confirming a close relatedness between them. It is suggested that phage 41c be included in Group 5 of B. subtilis bacteriophages (26). Phage SPP1 is presently the sole member of this group.

Physiological data revealed that phage 41c is a highly virulent phage for B. subtilis. Following a latent period of 50 min, there was a burst size of about 10^{3} phage per host cell. Phage 41c-directed protein synthesis was completed by 20 min post-infection. Nevertheless, host replication continued until lysis insued.

Infection of B. subtilis 168 by phages 41c or SPP1 resulted in ultrastructural changes which were not reported in previous ultrastructural studies of phage-infected cells. In the present

study, a marked rearrangement of the mesosomes was seen. Distinct changes in these structures were noted in cells prepared for transmission electron microscopy by two different procedures. Cells infected with the dissimilar phage SP82G, did not exhibit such ultrastructural changes. Protein synthesis on membrane surfaces could not account for these changes since they were observed subsequent to treatment with chloramphenicol. Since all phage DNA is probably membrane associated, DNA synthesis was also eliminated as a cause of mesosome alterations. Although it is possible that phage assembly was directly associated with membrane surfaces, protoplast formation never revealed phage within the extruded mesosomes.

Results of energy dispersive X-ray analysis clearly showed a decrease in cellular potassium and phosphorous of the infected cells as compared to the uninfected cells. This ionic change was probably a result of damaged membranes caused by phage infection. Thus, it seems likely that the rearrangement of mesosomes was influenced by the ionic composition within the cells.

APPENDIX

APPENDIX

Gene assignments and molecular weights of SPP1 proteins

Gene	Molecular Weights of Peptides (daltons)	Structural Proteins (+)
E1	124,000	
E2	61,000	
E3	55,000	
M10	120,000	
M11	83,000	+
M12	95,000	+
M13	42,000	+
M14	17,000	+
M15	48,000	+
M16	11,000	+
M17	13,000	+
M18	39,000	+
M19	30,000	+
M20	35,000	+
M21	23,000	
M22	32,000	
M23	21,000	
L30	51,000	
L31	98,000	
L32	103,000	
L33	71,000	
$C_{(x)}$	53,000	
$C_{(y)}$	28,500	

Esche, H. et al. (33)

LITERATURE CITED

LITERATURE CITED

1 Adams, M.H. 1959. Bacteriophages. Interscience Publishers, Inc., New York.

2 Bespalova, I.A., N.N. Belyaeva, S.Y. Medvedeva, and A.S. Tikhonenko. 1973. Intracellular development of phage AR7 of Bacillus subtilis. Microbiology 42:807-812.

3 Bespalova, I.A., L.N. Moskalenko, Y.I. Rautenshtein, and A.S. Tikhonenko. 1976. Electron microscopic study of the intracellular development of a phage specific for Bacillus thuringiensis var. galleriae. Microbiology 45:759-763.

4 Bhacca, N.S., D.P. Hollis, L.F. Johnson, and E.A. Pier. 1963. Nuclear Magnetic Resonance Spectra Catalog, Vol. 2. Varian Associates.

5 Bijlenga, R.K.L., D. Scraba, and E. Kellenberger. 1973. Studies on the morphopoiesis of the head of T-even phage. IX. T-particles: their morphology, kinetics of appearance and possible precursor functions. Virology 56:250-267.

6 Bradford, M.M. 1976. A rapid and sensitive method for the quantitation of protein utilizing the principles of protein-dye binding. Anal. Biochem. 72:248-254.

7 Bradley, D.E., and C.A. Dewar. 1967. Intracellular changes in cells of Escherichia coli infected with a filamentous bacteriophage. J. Gen. Virol. 1:179-188.

8 Bradley, D.E., and J.F.M. Hoeniger. 1971. Structural changes in cells of Clostridium perfringens infected with a short-tailed bacteriophage. Can. J. Microbiol. 17:397-402.

9 Brenner, S., and G.S. Stent. 1955. Bacteriophage growth in protoplasts of Bacillus megaterium. Biochim. Biophys. Acta. 17:473-475.

10 Burdett, I.D.J., and H.J. Rogers. 1970. Modification of the appearance of mesosomes in sections of Bacillus licheniformis according to the fixation procedures. J. Ultrastruct. Res. 30:354-367.

11 Burdett, I.D.J., and H.J. Rogers. 1972. The structure and development of mesosomes studied in Bacillus licheniformis strain 6346. J. Ultrastruct. Res. 38:113-133.

12 Carrascosa, J.L., and E. Kellenberger. 1978. Head maturation pathway of bacteriophages T4 and T2. III. Isolation and characterization of particles produced by mutants in gene 17. J. Virology 25:831-844.

13 Christian, J.H.B., and J.A. Waltho. 1962. Solute concentrations within cells of halophilic and nonhalophilic bacteria. Biochim. Biophys. Acta. 65:506-508.

14 Davis, B.J. 1964. Disc electrophoresis. II. Method and application to human serum proteins. Ann. N.Y. Acad. Sci. 121: 404-427.

15 Ebersold, H.R., J.L. Cordier, and P. Lüthy. 1981. Bacterial mesosomes: Method dependent artifacts. Arch. Microbiol. 130: 19-22.

16 Esche, H. 1975. Gene expression of bacteriophage SPP1. II. Regulatory aspects. Molec. Gen. Genet. 142:57-66.

17 Esche, H., M. Schweiger, and T.A. Trautner. 1975. Gene expression of bacteriophage SPP1. I. Phage directed protein synthesis. Molec. Gen. Genet. 142:45-55.

18 Fitz-James, P.C. 1960. Participation of the cytoplasmic membrane in the growth and spore formation of bacilli. J. Biophys. Biochem. Cytol. 8:507-528.

19 Fitz-James, P.C. 1964. Fate of the mesosomes of Bacillus megaterium during protoplasting. J. Bacteriol. 87:1483-1491.

20 Fooke-Achterrath, M., K.G. Lickfeld, V.M. Reusch, Jr., U. Abei, U. Tschöpe, and B. Menge. 1974. Close-to-life preservation of Staphylococcus aureus mesosomes for transmission electron microscopy. J. Ultrastruct. Res. 49:270-285.

21 Fuller, M.T., and J. King. 1980. Regulation of coat protein polymerization by the scaffolding protein of bacteriophage P22. Biophys. J. 10:381-401.

22 Ghosh, B.K., and N. Nanninga. 1976. Polymorphism of the mesosome in Bacillus licheniformis (749/C and 749). Influence of chemical fixation monitored by freeze-etching. J. Ultrastruct. Res. 56:107-120.

23 Green, D.M. 1964. Infectivity of DNA isolated from Bacillus subtilis bacteriophage SP82. J. Mol. Biol. 10:438-451.

24 Greenawalt, J.W., and T.L. Whiteside. 1975. Mesosomes: Membranous bacterial organelles. Bacteriol. Rev. 39:405-463.

25 Haberer, K., J. Maniloff, and D. Gerling. 1980. Adsorption, capping, and release of a complex bacteriophage by mycoplasma cells. J. Virology 36:264-270.

26 Hemphill, H.E., and H.R. Whiteley. 1975. Bacteriophages of Bacillus subtilis. Bacteriol. Rev. 39:257-315.

27 Higgins, M.L., H.C. Tsien, and L. Daneo-Moore. 1976. Organization of mesosomes in fixed and unfixed cells. J. Bacteriol. 127:1519-1523.

28 Highton, P.J., J. Lloyd, and M. Whitfield. 1973. Mesosomes of Bacillus subtilis, seen by negative staining. J. Gen. Microbiol. 78:375-378.

29 Humphreys, G.O., and T.A. Trautner. 1981. Maturation of bacteriophage SPP1 DNA: Limited precision in the sizing of the mature bacteriophage genomes. J. Virology 37:832-835.

30 Humphreys, G.O., and T.A. Trautner. 1981. Structure of Bacillus subtilis bacteriophage SPP1 DNA in relation to its transfection activity. J. Virology 37:574-579.

31 Ivarie, R.D., and J.J. Pene. 1973. DNA replication in bacteriophage Ø29: the requirement of a viral-specific product for association of Ø29 DNA with the cell membrane of Bacillus amyloliquefaciens. Virology 52:351-362.

32 Jacobson, E.D., and O.E. Landman. 1975. Interaction of protoplasts, L forms, and bacilli of Bacillus subtilis with 12 strains of bacteriophage. J. Bacteriol. 124:445-458.

33 Kallen, R.G., M. Simon, and J. Marmur. 1962. The occurrence of a new pyrimidine base replacing thymine in a bacteriophage DNA: 5-hydroxymethyl uracil. J. Mol. Biol. 5:248-250.

34 Kawakami, M., and O.E. Landman. 1968. On the nature of the carrier state of phage SP-10 in Bacillus subtilis. J. Bacteriol. 95:1804-1812.

35 Kaye, J.J., and G.B. Chapman. 1963. Cytological aspects of antimicrobial antibiosis. III. Cytologically distinguishable stages in antibiotic action of colistin sulfate on Escherichia coli. J. Bacteriol. 86:536-543.

36 Kellenberger, E., F.A. Eiserling, and E. Boy de la Tour. 1968. Studies on the morphopoiesis of the head of phage T-even. III. The cores of head-related structures. J. Ultrastruct. Res. 21:335-360.

37 Kellenberger, E., A. Ryter, and J. Sechaud. 1958. Electron microscope study of DNA-containing plasms. II. Vegetative and mature phage DNA as compared with normal bacterial nucleoids in different physiological states. J. Biophys. Biochem. Cytol. 4:671-687.

38 Klotz, G., and H. Ch. Spatz. 1971. A biological assay for intracellular SPP1 DNA. Molec. Gen. Genet. 110:367-373.

39 Laemmli, U.K. 1970. Cleavage of structural proteins during the assembly of the head of bacteriophage T4. Nature 227: 680-685.

40 Landry, E.F. 1975. Effect of Ca^{++} on the lytic cycle of bacteriophage 41c. Doctoral Dissertation, Department of Microbiology, University of New Hampshire, Durham, N.H.

41 Landry, E.F., and R.M. Zsigray. 1980. Effects of calcium on the lytic cycle of Bacillus subtilis phage 41c. J. Gen. Virol. 51:125-135.

42 Lencastre, H., and L.J. Archer. 1980. Characterization of bacteriophage SPP1 transducing particles. J. Gen. Microbiol. 117:347-355.

43 Liljemark, W.F., and D.L. Anderson. 1970. Morphology and physiology of the intracellular development of Bacillus subtilis bacteriophage ϕ25. J. Virology 6:114-124.

44 Mandel, J.D., and A.D. Hershey. 1960. A fractionating column for analysis of nucleic acids. Anal. Biochem. 1:66-77.

45 Maniloff, J., J. Das, R.M. Putzrath, and J.A. Nowak. 1979. Mycoplasma and spiroplasma viruses: Molecular biology, p. 411-430. In M.F. Barile and S. Razin (eds.), The Mycoplasmas, Vol. I. Academic Press, Inc., New York.

46 Matheson, A., M.K. Yang, and R.P. Smith. 1973. Demonstration of ribosomes in mesosomes associated with Bacillus subtilis protoplasts. J. Bacteriol. 115:349-357.

47 Milanesi, G., and G. Cassani. 1972. Transcription after bacteriophage SPP1 infection in Bacillus subtilis. J. Virology 10:187-192.

48 Miller, I.L., R.M. Zsigray, and O.E. Landman. 1967. The formation of protoplasts and quasi-spheroplasts in normal and chloramphenicol-pretreated Bacillus subtilis. J. Gen. Microbiol. 49:513-525.

49 Montenegro, A., H. Esche, and T.A. Trautner. 1976. Induction of mutations in Bacillus subtilis phage SPP1. Growth on host cells carrying a mutator DNA polymerase III. Molec. Gen. Genet. 149:131-134.

50 Nanninga, N. 1971. The mesosome of Bacillus subtilis as affected by chemical and physical fixation. J. Cell Biol. 48:219-224.

51 Nanninga, N., L.J.H. Koppes, and F.C. de Vries-Tijssen. 1979. The cell cycle of Bacillus subtilis as studied by electron microscopy. Arch. Microbiol. 123:173-181.

52 Nelson, R.A., B.E. Reilly, and D.L. Anderson. 1976. Morphogenesis of bacteriophage Ø29 of Bacillus subtilis: Preliminary isolation and characterization of intermediate particles of the assembly pathway. J. Virology 19:518-532.

53 Ohnishi, Y., and M. Kuwano. 1971. Growth inhibition and appearance of the membranous structure in Escherichia coli infected with bacteriophage fd. J. Virology 7:673-678.

54 Okubo, S., B. Strauss, and M. Stodolsky. 1964. The possible role of recombination in the infection of competent Bacillus subtilis by bacteriophage deoxyribonucleic acid. Virology 24: 552-562.

55 Ornstein, L. 1964. Disc electrophoresis. I. Background and theory. Ann. N.Y. Acad. Sci. 121:321-349.

56 Palefski, S., H.E. Hemphill, P.E. Kolenbrander, and H.R. Whiteley. 1972. Dominance relationships in mixedly infected Bacillus subtilis. J. Virology 9:594-601.

57 Parks, L.C., D.T. Dicker, A.D. Conger, L. Daneo-Moore, and M.L. Higgins. 1981. Effect of chromosomal breaks induced by X-irradiation on the number of mesosomes and the cytoplasmic organization of Streptococcus faecalis. J. Mol. Biol. 146:413-431.

58 Persi, M.A., and R.M. Pfister. 1978. A quantitative analysis of the effects of three environmental gases on the appearance of mesosomes in Bacillus subtilis. Micron 9:43-44.

59 Pontefract, R.D., G. Bergeron, and F.S. Thatcher. 1969. Mesosomes in Escherichia coli. J. Bacteriol. 97:367-375.

60 Razzell, W.E., and H.G. Khorana. 1959. Studies on polynucleotides. IV. Enzymic degradation. The stepwise action of venom phosphodiesterase on deoxyribo-oligonucleotides. J. Biol. Chem. 234:2114-2117.

61 Reilly, B.E., and J.Spizizen. 1965. Bacteriophage deoxyribonucleate infection of competent Bacillus subtilis. J. Bacteriol. 89:782-790.

62 Reynolds, E.S. 1963. The use of lead citrate at high pH as an electron-opaque stain in electron microscopy. J. Cell Biol. 17:208-212.

63 Riva, S., and M. Polsinelli. 1968. Relationship between competence for transfection and transformation. J. Virology 2:587-593.

64 Riva, S., M. Polsinelli, and A. Falaschi. 1968. A new phage of Bacillus subtilis with infectious DNA having separable strands. J. Mol. Biol. 35:347-356.

65 Roscoe, D.H. 1969. Synthesis of DNA in phage-infected Bacillus subtilis. Virology 38:527-537.

66 Rucinsky, T.E., and E.H. Cota-Robles. 1974. Mesosome structure in Chromobacterium violaceum. J. Bacteriol. 118:717-724.

67 Ryter, A., and F. Jacob. 1966. Étude morphologique de la liaison du noyau a la membrane chez E. coli et chez les protoplastes de B. subtilis. Ann. Inst. Pasteur (Paris) 110:801-812.

68 Sadtler Research Laboratories. 1974. The Sadtler Standard Nuclear Magnetic Resonance Spectra. Vol. 28. Philadelphia, Pa.

69 Salton, M.R.J., and M. McQuillen. 1955. Bacterial protoplasts. II. Bacteriophage multiplication in protoplasts of sensitive and lysogenic strains of Bacillus megaterium. Biochim. Biophys. Acta. 17:465-472.

70 Schachtele, C.F., R.W. Orman, and D.L. Anderson. 1970. Effect of elevated temperature on deoxyribonucleic acid synthesis in bacteriophage Ø29-infected Bacillus amyloliquefaciens. J. Virology 6:430-437.

71 Schaerli, C., and E. Kellenberger. 1980. Head maturation pathway of bacteriophages T4 and T2. V. Maturable Σ-particles accumulating in acridine-treated bacteriophage T4-infected cells. J. Virology 33:830-844.

72 Schwartz, F.M., and N.D. Zinder. 1967. Morphological changes in Escherichia coli infected with the DNA bacteriophage f1. Virology 34:352-355.

73 Silva, M.T. 1971. Changes induced in the ultrastructure of the cytoplasmic and intracytoplasmic membranes of several Gram-positive bacteria by variations in OsO_4 fixation. J. Micros. 93:227-232.

74 Silva, M.T., and J.C.F. Sousa. 1972. Ultrastructural alterations induced by moist heat in Bacillus cereus. Appl. Microbiol. 24:463-476.

75 Simon, L.D. 1972. Infection of Escherichia coli by T2 and T4 bacteriophages as seen in the electron microscope: T4 head morphogenesis. Proc. Natl. Acad. Sci. (U.S.A.) 69: 907-911.

76 Spatz, H.C., and T.A. Trautner. 1970. One way to do experiments on gene conversion: Transfection with heteroduplex SPP1 DNA. Molec. Gen. Genet. 109:84-106.

77 Spatz, H. Ch., and T.A. Trautner. 1971. The role of recombination in transfection of B. subtilis. Molec. Gen. Genet. 113:174-190.

78 Spurr, A.R. 1969. A low-viscosity epoxy resin embedding medium for electron microscopy. J. Ultrastruct. Res. 26: 31-43.

79 Stanier, R.Y., E.A. Adelberg, and J. Ingraham. 1976. The Microbial World. 4th Ed. Prentice-Hall, Inc., Englewood Cliffs, N.J.

80 Steensma, H.Y., and J. Blok. 1979. Effect of calcium ions on the infection of Bacillus subtilis by bacteriophage SF6. J. Gen. Virol. 42:305-314.

81 Tikhonenko, A.S., and I.A. Bespalova. 1964. Phage maturation in Bacillus mycoides cells. Virology 23:259-267.

82 Van Iterson, W., and J.A. Aten. 1976. Nuclear and cell division in Bacillus subtilis: Cell development from spore germination. J. Bacteriol. 126:384-399.

83 Van Iterson, W., P.A.M. Michels, F. Vyth-Dreese, and J.A. Aten. 1975. Nuclear and cell division in Bacillus subtilis: Dormant nucleotides in stationary-phase cells and their activation. J. Bacteriol. 121:1189-1199.

84 Weber, K., and M. Osborn. 1969. The reliability of molecular weight determinations by dodecyl sulfate-polyacrylamide gel electrophoresis. J. Biol. Chem. 244:4406-4412.

85 Woese, C.R., J. Maniloff, and L.B. Zablen. 1980. A phylogenetic analysis of the mycoplasmas. Proc. Natl. Acad. Sci. (U.S.A.) 77:494-498.

86 Wyatt, G.R. 1951. The purine and pyrimidine composition of deoxypentose nucleic acids. Biochem. J. 48:584-590.

87 Wyatt, G.R., and S.S. Cohen. 1953. The base of the nucleic acids of some bacterial and animal viruses: The occurrence of 5-hydroxymethylcytosine. Biochem. J. 55:774-782.

88 Wyckoff, R.W.G. 1948. The electron microscope of developing bacteriophage. II. Growth of T4 in liquid culture. Biochim. Biophys. Acta. 2:246-253.

89 Yasbin, R.E., and F.E. Young. 1974. Transduction in Bacillus subtilis by bacteriophage SPP1. J. Virology 14:1343-1348.

90 Yehle, C.O., and R.H. Doi. 1967. Differential expression of bacteriophage genomes in vegetative and sporulating cells of Bacillus subtilis. J. Virology 1:935-947.

91 Yehle, C.O., and A.T. Ganesan. 1972. Deoxyribonucleic acid synthesis in bacteriophage SP01-infected Bacillus subtilis. I. Bacteriophage deoxyribonucleic acid synthesis and fate of host deoxyribonucleic acid in normal and polymerase-deficient strains. J. Virology 9:263-272.

92 Zsigray, R.M. 1968. The penetration of a bacteriophage into Bacillus subtilis. Doctoral Dissertation, Department of Biology, Georgetown University, Washington, D.C.

93 Zsigray, R.M., A.L. Miss, and O.E. Landman. 1973. Penetration of a bacteriophage into Bacillus subtilis: Blockage of infection by deoxyribonuclease. J. Virology 11: 69-77.